

X
BNL-NCS-51028
(ENDF-279)

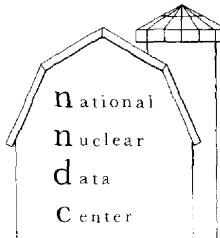
ENDF/B-V NEUTRON
CROSS SECTION EVALUATION
FOR THE KRYPTON ISOTOPES

A. PRINCE

January 1979

INFORMATION ANALYSIS CENTER REPORT

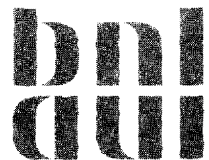
NATIONAL NUCLEAR DATA CENTER
BROOKHAVEN NATIONAL LABORATORY
UPTON, NEW YORK 11973



BNL-NCS-51028
(ENDF-279)
UC-34c
(Physics-Nuclear - TID-4500)

ENDF/B-V NEUTRON CROSS SECTION
EVALUATION FOR THE KRYPTON ISOTOPES

A. PRINCE



January 1979

NATIONAL NUCLEAR DATA CENTER
BROOKHAVEN NATIONAL LABORATORY
ASSOCIATED UNIVERSITIES, INC.
UNDER CONTRACT NO. EY-76-C-0016 WITH THE
UNITED STATES DEPARTMENT OF ENERGY

N O T I C E

This report was prepared as an account of work sponsored by the United States Government. Neither the United States nor the United States Department of Energy (DOE), nor any of their employees, nor any of their contractors, subcontractors, or their employees, makes any warranty, express or implied, or assumes any legal liability or responsibility for the accuracy, completeness or usefulness of any information, apparatus, product or process disclosed, or represents that its use would not infringe privately owned rights.

Printed in the United States of America
Available from
National Technical Information Service
U.S. Department of Commerce
5285 Port Royal Road
Springfield, VA 22161
Price: Printed Copy \$5.25; Microfiche \$3.00

August 1979 485 copies

ABSTRACT

This report describes the evaluation of the neutron cross-section data for the six stable isotopes of Kr from 10^{-5} eV to 20 MeV. These evaluations incorporate all the new data on these isotopes including those on the resonance parameters, level schemes of the various isotopes and residual nuclei and reaction data. Evaluation procedures adopted to assess experimental data and the nuclear model calculations used are described.

	CONTENTS	Page
1.0	Introduction	1
2.0	Resonance Region	1
3.0	Continuum Region Cross Section	4
4.0	Angular Distribution of Secondary Neutrons	4
5.0	Energy Distribution of Secondary Neutrons	5
	Acknowledgments	5
	References	5
	TABLES	
1	Adopted Resonance Parameters	6
2	Experimental and Recommended Thermal Capture Cross Sections for ^{80}Kr .	6
3	Natural Abundance and Mass of Krypton Isotopes	7
4	Optical Model Potential	7
5	Q Values for Nuclear Reactions	7
6(a)	Energy Levels for Hauser-Feshbach Calculations: ^{78}Kr	8
6(b)	Energy Levels for Hauser-Feshbach Calculations: ^{80}Kr	8
6(c)	Energy Levels for Hauser-Feshbach Calculations: ^{82}Kr	9
6(d)	Energy Levels for Hauser-Feshbach Calculations: ^{83}Kr	9
6(e)	Energy Levels for Hauser-Feshbach Calculations: ^{84}Kr	10
6(f)	Energy Levels for Hauser-Feshbach Calculations: ^{86}Kr	10

FIG.	LIST OF FIGURES	Page
1	^{78}Kr Total Neutron Cross Section in the Resonance Region	11
2	^{78}Kr Elastic Neutron Cross Section in the Resonance Region	11
3	^{78}Kr Capture Neutron Cross Section in the Resonance Region	12
4	^{80}Kr Total Neutron Cross Section in the Resonance Region	12
5	^{80}Kr Elastic Neutron Cross Section in the Resonance Region	13
6	^{80}Kr Capture Neutron Cross Section in the Resonance Region	13
7	^{82}Kr Total Neutron Cross Section in the Resonance Region	14
8	^{82}Kr Elastic Neutron Cross Section in the Resonance Region	14
9	^{82}Kr Capture Neutron Cross Section in the Resonance Region	15
10	^{83}Kr Total Neutron Cross Section in the Resonance Region	15
11	^{83}Kr Elastic Neutron Cross Section in the Resonance Region	16
12	^{83}Kr Capture Neutron Cross Section in the Resonance Region	16
13	^{84}Kr Total Neutron Cross Section in the Resonance Region	17
14	^{84}Kr Elastic Neutron Cross Section in the Resonance Region	17
15	^{84}Kr Capture Neutron Cross Section in the Resonance Region	18
16	^{86}Kr Total Neutron Cross Section in the Resonance Region	18
17	^{86}Kr Elastic Neutron Cross Section in the Resonance Region	19
18	^{86}Kr Capture Neutron Cross Section in the Resonance Region	19
19	$\text{Kr}(\text{Nat})$ Total Neutron Cross Section (0.002 to 10.0 eV)	20
20	$\text{Kr}(\text{Nat})$ Total Neutron Cross Section (10.0 eV to 100.0 keV)	21
21	$\text{Kr}(\text{Nat})$ Total Neutron Cross Section (0.1 to 20.0 MeV)	22
22	$^{78}\text{Kr}(n,n')$ First Excited Neutron Cross Section ($Q = - 455.0$ keV)	23
23	$^{78}\text{Kr}(n,n')$ Continuum Neutron Cross Section	23
24	^{78}Kr Total Inelastic Neutron Cross Section	24
25	$^{78}\text{Kr}(n,p)$ Neutron Cross Section	24
26	$^{78}\text{Kr}(n,\alpha)$ Neutron Cross Section	25
27	$^{78}\text{Kr}(n,2n)$ Neutron Cross Section	25
28	^{78}Kr Non-elastic Neutron Cross Section	26
29	$^{80}\text{Kr}(n,n')$ First Excited Neutron Cross Section ($Q = - 616.0$ keV)	26
30	$^{80}\text{Kr}(n,n')$ Continuum Neutron Cross Section	27
31	^{80}Kr Total Inelastic Neutron Cross Section	27
32	$^{80}\text{Kr}(n,p)$ Neutron Cross Section	28
33	$^{80}\text{Kr}(n,\alpha)$ Neutron Cross Section	28
34	$^{80}\text{Kr}(n,2n)$ Neutron Cross Section	29
35	^{80}Kr Non-elastic Neutron Cross Section	29
36	$^{82}\text{Kr}(n,n')$ First Excited Neutron Cross Section	30
37	$^{82}\text{Kr}(n,n')$ Continuum Neutron Cross Section	30
38	^{82}Kr Total Inelastic Neutron Cross Section	31
39	$^{82}\text{Kr}(n,p)$ Neutron Cross Section	31
40	$^{82}\text{Kr}(n,\alpha)$ Neutron Cross Section	32
41	$^{82}\text{Kr}(n,2n)$ Neutron Cross Section	32
42	^{82}Kr Non-elastic Neutron Cross Section	33
43	$^{83}\text{Kr}(n,n')$ First Excited Neutron Cross Section ($Q = - 9.4$ keV)	33
44	$^{83}\text{Kr}(n,n')$ Continuum Neutron Cross Section	34
45	^{83}Kr Total Inelastic Neutron Cross Section	34
46	$^{83}\text{Kr}(n,p)$ Neutron Cross Section	35
47	$^{83}\text{Kr}(n,\alpha)$ Neutron Cross Section	35
48	$^{83}\text{Kr}(n,2n)$ Neutron Cross Section	36
49	$^{83}\text{Kr}(n,3n)$ Neutron Cross Section	36

	Figures (cont'd)	Page
50	^{83}Kr Non-elastic Neutron Cross Section	37
51	$^{84}\text{Kr}(n,n')$ First Excited Neutron Cross Section ($Q = - 882.0$ keV)	37
52	$^{84}\text{Kr}(n,n')$ Continuum Neutron Cross Section	38
53	^{84}Kr Total Inelastic Neutron Cross Section	38
54	$^{84}\text{Kr}(n,p)$ Neutron Cross Section	39
55	$^{84}\text{Kr}(n,\alpha)$ Neutron Cross Section	39
56	$^{84}\text{Kr}(n,2n)$ Neutron Cross Section	40
57	^{84}Kr Non-elastic Neutron Cross Section	40
58	$^{86}\text{Kr}(n,n')$ First Excited Neutron Cross Section ($Q = - 1.563$ MeV)	41
59	$^{86}\text{Kr}(n,n')$ Continuum Neutron Cross Section	41
60	^{86}Kr Total Inelastic Neutron Cross Section	42
61	$^{86}\text{Kr}(n,p)$ Neutron Cross Section	42
62	$^{86}\text{Kr}(n,2n)$ Neutron Cross Section	43
63	$^{86}\text{Kr}(n,3n)$ Neutron Cross Section	43
64	^{86}Kr Non-elastic Neutron Cross Section	44
65	Kr(Nat) Capture Neutron Cross Section (10^{-5} eV to 20.0 MeV)	45
66	Kr(Nat) Elastic Neutron Cross Section (10^{-5} eV to 20.0 MeV)	46
67	Kr(Nat) Total Neutron Cross Section (10^{-5} eV to 20.0 MeV)	47

1.0 INTRODUCTION

Because of the importance of krypton as a tag material for detecting and locating fuel failure in the FFTF,¹ the decision was made to upgrade the evaluation for the six stable isotopes for inclusion in ENDF/B-V. The major differences between the ENDF/B-IV¹ evaluation and the new one are related to the recent experimental resonance parameter data of Block et al.² New data on the level schemes of the various isotopes and residual nuclei resulting from neutron interactions also prompted a more detailed treatment of the various reaction cross sections. The evaluation covers all significant possible neutron-induced reactions from 10^{-5} eV to 20.0 MeV.

The isotopes and their corresponding MAT numbers are given below for ENDF/B-V.

Isotope	MAT
^{78}Kr	1330
^{80}Kr	1331
^{82}Kr	1332
^{83}Kr	1333
^{84}Kr	1334
^{86}Kr	1336

2.0 RESONANCE REGION

^{78}Kr MAT (10^{-5} eV to 865.0 eV)

The recent experimental data of Block et al.,² were used for calculating the cross section and resonances integral in this energy region. Block et al., concluded the ^{78}Kr and ^{80}Kr form a doublet around $E = 106.0$ eV, an assumption that was made in ENDF/IV. In addition, since neither Block² nor Mann and Watson³ could definitely assign the 640-eV level to any particular isotope, although they designated the possibilities to be ^{78}Kr , ^{80}Kr ,^{1,3} and a doublet in ^{82}Kr ,² this resonance was used in both ^{78}Kr and ^{80}Kr .

A negative resonance at $E_R = -120.6$ eV produced a thermal capture cross section

$$\sigma(0.0253 \text{ eV}) = 4.85 \text{ b}$$

which compares favorably with the experimental

$$\sigma(0.0253 \text{ eV}) = 4.71 \pm 0.68 \text{ b}^{4,5}$$

There are no experimental data for the absorption resonance integral for ^{78}Kr . The calculated value, based on the resonance parameters given in Table 1, is $I_{ab}^{ab} (E_{cutoff} = 0.5 \text{ eV}) = 23.67 \text{ b}$. Block et al., estimated that $I_{ab}^{ab} = 20.0 \pm 1.0 \text{ b}$ between 20.0 and 1200.0 eV. Both these values are about five times as large as the value quoted in Ref. 6, the reason being that in Ref. 6 only the 640.0-eV resonance was used.

Figures 1 to 3 shows the calculated values of the total, scattering, and capture cross sections, in the resonance region, based on the single-level Breit-Wigner formalism. The potential scattering cross section was estimated

to be 7.00 b on the basis of several measurements ranging from 6.2 ± 0.1 b⁷ to 7.61 ± 0.04 b⁸ (also see Refs. 6 and 9) for Kr(Nat).

^{80}Kr MAT 1331 (10⁻⁵ eV to 1.0 keV)

Use of the resonance parameters shown in Table 1, where a bound level is located $E = -118.0$ eV, yielded a thermal capture cross section $\sigma_{\text{ny}} = 11.74$ b, which may be compared with the range of values given in Table 2.

The resonance integral calculated by using the parameters in Table 1 produced a value of I (0.5-eV cutoff) = 68.6 b, which, although somewhat higher than those recommended in Refs. 2, 6, and 10, is preferred since the most recent quoted value² is based on data in the region 20.0 to 1200.0 eV which clearly underestimate the evaluated value that goes from 0.05 eV to the MeV range.

The potential scattering cross section is taken to be the same as that of ^{78}Kr .

The total, elastic, and capture cross sections in the resonance regions are shown in Figures 4 to 6.

^{82}Kr MAT 1332 (10⁻⁵ eV to 100.0 eV)

Only one resonance at an energy of ~ 40 eV has been firmly established for ^{82}Kr .^{2,6} Block et al.,² have concluded that there is a doublet belonging to ^{82}Kr around 640.0 eV, but, since they give no neutron width (Γ_n), this resonance has been ignored.

The radiation width $\Gamma_{\gamma\gamma}$ was determined by the method proposed by Malecky et al.,¹¹ in which it is assumed that the main contribution to $\Gamma_{\gamma\gamma}$ is due to the electric dipole radiation; from a semi-empirical analysis it may be estimated as

$$\Gamma_{\gamma\gamma} = 10.5 U/A (a^{-1/2}) (1.0 - 0.01 I^2) \text{ eV} \quad (1)$$

where

A = mass of nucleus,

U = effective energy of excitation ($U = E_B - \Delta$),

E_B = binding energy of compound nucleus,

Δ = $\delta(N)$ and $\delta(p)$ the pairing energies,

I = spin of target nucleus, and

a = single-particle state density parameter near the Fermi surface.

The relation between a and A is based on the analysis of Cook et al.,¹² where

$a/A = 0.00917S + 0.142$, and

$S = S(N) + S(Z)$ shell correction parameter.

A value of $\Gamma_{\gamma\gamma} = 236$ mV was calculated from Eq. (1) for ^{82}Kr .

In addition to the reported resonance at 39.8 eV, it was necessary to assume a bound level at -42.83 eV (Table 1) to yield a thermal capture cross section $\sigma_{\text{ny}} = 30.17$ b. The experimental value leading to the metastable state in ^{83}Kr of $\sigma_{\text{ny}}^m = 20.0 \pm 3.5$ b has been reported in Ref. 4. The value calculated here is barely within the recommended value of

$\sigma_{n\gamma}^{(m+g)} = 45 \pm 15$ b.⁶ A value $\sigma_{n\gamma} = 25.0$ b has been estimated by Iijima.¹³

As with ^{78}Kr and ^{80}Kr , the potential scattering cross section was chosen to be $\sigma_{\text{pot}} = 7.0$ b.

The resonance integral calculated from the data in Table 1 is $I_\gamma = 183.56$ b ($E_{\text{cutoff}} = 0.5$ eV). The recommended value calculated from a single resonance at 39.8 eV has been given as 200 ± 40 b.⁶ A calculated $I_\gamma = 190.0$ b where 13.7 b is due to the unresolved region was reported in Ref. 13.

The total, elastic, and capture cross sections for the resonance region are displayed in Figures 7 through 9.

^{83}Kr MAT 1333 (10⁻⁵ to 520.625 eV)

The resonance parameters given in Ref. 3 yielded a thermal capture cross section of the only 16 b, which is much too small compared with the various recommended values 200 ± 30 b⁶ and 205 b.¹³

Calculating the radiation width by Eq. (1) yielded $\Gamma_{\gamma\gamma} = 233.0$ mV; assuming a bound level at -3.9 eV gives a thermal capture cross section $\sigma_{n\gamma} = 207.67$ b.

The calculated resonance integral is $I_\gamma = 188.65$ b, which is lower than the value $I_\gamma = 230 \pm 30$ b quoted in Ref. 6 but higher than the value $I_\gamma = 170.2$ b in Ref. 13.

As earlier, the potential scattering cross section is the same as that of Kr(Nat), namely 7.0 b.

Figures 10 through 12 show the total, elastic, and capture cross section from 1.0 eV to 1.0 keV.

^{84}Kr MAT 1334 (10⁻⁵ to 2.0 keV)

An unassigned resonance reported by Mann and Watson³ was assumed to be due to ^{84}Kr at an energy of 1625.0 eV, with a neutron width $\Gamma_n = 2.84.0$ mV and $\Gamma_\gamma = 226.0$ mV (Eq. 1). This resonance along with the other two low-lying resonances at 519.0 and 580.0 eV yielded a thermal capture cross section $\sigma_{n\gamma}(0.0253 \text{ eV}) = 0.0864$ b. Kondaiah et al.,⁴ reported an experimental value of 0.09 ± 0.013 b for the 4.4-h ^{85}Kr and a value of 0.042 ± 0.004 b for the 10.74- γ ^{85}Kr . A recommended value of $\sigma_{n\gamma} = 0.130 \pm 0.014$ b $^{85}\text{Kr}^{(m+g)}$ is given in Ref. 6, and $\sigma_{n\gamma} = 0.16$ b is reported in Ref. 14.

The calculated resonance integral of magnitude 3.27 b is in good agreement with the calculated value of 2.7 ± 0.7 b reported in Ref. 6, and in excellent agreement with $I_\gamma = 3.54$ given in Ref. 14.

The total, elastic, and capture cross sections are given in Figures 13 to 15.

^{86}Kr MAT 1336 (10^{-5} eV to 13 keV)

Since no resonance parameters have been experimentally verified for ^{86}Kr , it was necessary to make certain assumptions. From Mann et al.,³ there is an unassigned resonance at an energy of ~ 2700 eV. Since the thermal capture cross section and resonance integral for ^{86}Kr have been estimated to be very small (see following references) this resonance was taken to be due to this isotope.

On the basis of an estimated s-wave strength function, $s_0 = 0.5 \times 10^{-4}$, and assuming $\Gamma_\gamma/\Gamma_n \ll 1$, the resonance parameters given in Table 1 were derived.

These parameters produced a thermal capture cross section equal to 0.0635 b, which is not too far from the value 0.06 ± 0.02 b⁶ and is consistent with the estimate of 0.062 b.¹⁴ Again, a potential scattering radius of 7.0 was used.

The resonance integral was calculated to be 0.122 b, which may be compared with the calculated value of 0.03 ± 0.03 b³, and 0.07 quoted in Ref. 14 (also see Ref. 13).

The resonance region cross sections are shown in Figures 16 to 18.

Kr(Nat) Data

The total cross sections for the Kr isotopes calculated by using the resonance parameters in Table 1 were weighted by the respective isotopic abundance (see Table 3) and combined to produce the Kr(Nat) data. These results are compared with experimental data in Figures 19 and 20.

3.0 CONTINUUM REGION CROSS SECTION

The cross sections (total, elastic, inelastic capture, n-proton, and n- ^4He) in the keV to 20-MeV region were calculated by using the code CERBERO-2.¹⁶ The sources for the various optical model potentials employed are given in Table 4. No experimental data are available for the total cross sections for the Kr isotopes, but data do exist for Kr(Nat).

The O.M. calculations for the various isotopes were weighted by their abundance (see Table 3) and combined to give a calculated σ_T for Kr(Nat). The experimental data are compared with these results in Figure 21.

The n, γ , n,n', n,p, and n- ^4He reaction calculations were carried out in the Hauser-Feshbach formalism with width fluctuation correction and with the Q values given in Table 5. The level schemes used in these calculations are given in Table 6 (these levels were taken from Ref. 22 unless otherwise stated). The calculations were then modified to take into account other threshold reaction cross section (n,2n, n,3n, n,d, n,t) which were calculated for ENDF/IV (see Ref. 1).

Figures 22 through 67 show some of the more important reaction cross sections, up to 20.0 MeV.

4.0 ANGULAR DISTRIBUTION OF SECONDARY NEUTRONS

The angular distribution of the elastically scattered neutrons was interpreted in terms of a Legendre polynomial fit using CHAD²⁶ for File 4.

For the inelastically scattered neutrons and the n,2n reactions, the distribution was assumed to be isotropic.

5.0 ENERGY DISTRIBUTION OF SECONDARY NEUTRONS

The energy distributions of neutrons due to the n,2n, n,3n, and continuum inelastic scattering were expressed in terms of a normalized probability distribution having an evaporation spectrum given by

$$f(E + E') = E'/I e^{-E'/\theta}$$

where I = normalization constant, and θ = nuclear temperature. The energy dependence of θ was formulated according to Gilbert and Cameron.²⁷

ACKNOWLEDGMENTS

The author would like to express his appreciation to the various members of NNDC who helped in this evaluation effort. In particular, the diligent assistance of Anthony Fuoco, Frances Scheffel, and Sol Pearlstein, who were very supportive in carrying out many of the model calculations and plotting the various graphs, is gratefully acknowledged. In addition, a word of thanks is in order to Prof. R.C. Block and his colleagues at RPI for providing the resonance parameter data prior to publication and to R.E. Schenter (HEDL) for bringing this information to my attention. Finally, an expression of gratitude is extended to F. Fabbri and G. Reffo (CNEN) for furnishing their code CERBERO.

REFERENCES

1. A. Prince, BNL-NCS-50503, 1974.
2. R.C. Block et al., Int. Conf., Harwell, England, 1978.
3. D.P. Mann and W.W. Watson, Phys. Rev. 116, 1516 (1959).
4. R. Kondaiah et al., Nucl. Phys. A120, 329 (1968).
5. F.W. Walker et al., G.E. Chart of Nuclides (12th ed.) 1977.
6. S.F. Mughabghab and D.I. Garber, BNL 325 (3rd ed.), Vol. 1, 1973.
7. D.C. Rorer et al., Nucl. Phys. A133, 410 (1969).
8. V.E. Krohn and G.R. Ringo, Phys. Rev. 148, 1303 (1966).
9. S.J. Cocking, J. Nucl. Eng. 6, 113 (1958).
10. J.G. Bradley and W.H. Johnson, NSE 47, 151 (1972).
11. H. Malecky et al., Sov. J. Nucl. Phys. 13, 133 (1971).
12. J.L. Cook, Austr. J. Phys. 20, 477 (1967).
13. S. Iijima et al., JAERI 1206 (1971).
14. H. Saketa et al., JAERI, 1194 1970.
15. R. Genin et al., J. Phys. Radium 24, 21 (1963).
16. F. Fabbri et al., CERBERO-2, RT/F1(77)6, 1977.
17. D. Wilmore and P.E. Hodgson, Nucl. Phys. 55, 673 (1964).
18. F.D. Becchetti and G.W. Greenlees, Phys. Rev. 182, 1190 (1969).
19. M. Makowska et al., Rpt. 735/PL, Inst. Nucl. Phys., Cracow, Poland, 1970.
20. V.P. Vlasenko et al., Sov. Prog. Nucl. Phys., 206 (1961).
21. F.J. Vaughn et al., Phys. Rev. 118, 683 (1960).
22. Nuclear Data Sheets, Series B, Vol. 15, Academic Press, New York, 1975.
23. B.K. Arora et al., Phys. Rev. C10, 2301 (1974).
24. S. Väisälä et al., Phys. Rev. C13, 372 (1976).

References (cont'd)

25. E.B. Flynn et al., Phys. Rev. C13, 568 (1976).
26. R.F. Berland, CHAD, NAA-SR-11231 (1965).
27. A. Gilbert and A.G.W. Cameron, Can. J. Phys. 43, 1446 (1965).

Table 1
Adopted Resonance Parameters

Isotope	E_R (eV)	Γ_T (mV)	Γ_n (mV)	Γ_γ (mV)	Ref.
^{78}Kr	-120.6*	936.0	706.0	230.0	-
	108.4	279.0	49.0	230.0	2
	450.9	460.0	230.0	230.0	2
	640.0	1730.0	1500.0	230.0	2
^{80}Kr	-118.0*	1460.0	1230.0	230.0	-
	89.2	234.0	4.0	230.0	2
	106.0	670.0	440.0	230.0	2
	927.0	2530.0	2300.0	230.0	2
^{82}Kr	-42.83	496.0	260.0	236.0	1
	39.80	324.3	88.3	236.0	1
^{83}Kr	-3.9	245.44	12.44	233.0	1
	27.9	300.0	67.0	233.0	1
	233.0	523.0	290.0	233.0	1
^{84}Kr	519.0	571.0	345.0	226.0	1
	580.0	313.0	87.0	226.0	1
	1625.0	2410.0	2184.0	226.0	1
^{86}Kr	2730.0	3568.0	3400.0	168.0	1

*See text.

Table 2
Experimental and Recommended Thermal Capture Cross Sections for ^{80}Kr

σ_{ny} (b)	Reference
14.0±1.5	BNL 325, Vol. 1 (3rd ed.), 1973.
11.3±0.4	G. Bondley and W.H. Johnson, NSE 47, 151 (1972).
15.6±2.8	I.R. Barabanov et al., JETP Lett. 15, 456 (1972).
11.5±0.6	N.E. Holden and F.W. Walker, G.E. Chart of Nuclides (11th ed.), 1972.
11.5±0.5	N.E. Holden (BNL), Private Communication, 1978.
12.6	F.W. Walker et al., G.E. Chart of Nuclides (12th ed.), 1977.
11.74	This work.

Table 3
Natural Abundance and Mass of Krypton Isotopes

Isotope	% Abundance	Mass (amu)	S_n (MeV)*
78	0.35	77.920401	8.368
80	2.25	79.916376	7.850
82	11.60	81.913482	7.467
83	11.50	82.914131	10.518
84	57.00	83.911506	7.111
86	17.30	85.910616	5.511

* S_n = Binding energy of last neutron in compound nucleus.

Table 4
Optical Model Potential

Reaction	Reference
n,n	Wilmore and Hodgson ¹⁷
n,p	Becchetti and Greenlees ¹⁸
n, α	Makowska ¹⁹

Table 5
 Q Values for Nuclear Reactions

Reaction	78_{Kr}	80_{Kr}	82_{Kr}	83_{Kr}	84_{Kr}	86_{Kr}	ENDF
	-Q (MeV)	MT					
(n,p)	-0.089	1.228	2.306	0.187	3.920	6.520	103
(n, ^3He)	5.752	7.730	9.695	10.461	11.707	14.202	106
(n,n'd)	17.129	17.581	17.884	15.151	18.067	18.669	
(n,n' ^4He)	4.358	5.066	5.990	6.479	7.101	7.511	22
(n, $^4\text{He},n'$)	4.358	5.066	5.990	6.479	7.101	7.511	22
(n,p, ^4He)	4.931	7.252	5.990	7.942	12.322	14.308	
(n,2n)	11.981	11.525	10.980	7.467	10.518	9.860	16
(n,d)	5.974	6.886	7.766	7.548	8.480	9.655	104
(n, $^4\text{He})$	-3.665	0.969	-1.111	-1.526	-1.168	-1.384	107
(n,n't)	19.942	19.610	19.468	19.052	19.410	19.194	
(n,p,n')	8.199	9.111	9.907	9.773	10.705	11.880	28
(n, $^4\text{He},p)$	4.931	7.252	9.475	7.942	12.322	14.208	
(n,3n)	21.14	19.893	18.839	18.450	17.985	16.971	71
(n,t)	10.87	11.322	11.585	8.892	11.808	12.410	105
(n,n'p)	8.199	9.111	9.907	9.773	10.705	11.880	28
(n,n' ^3He)	16.913	18.226	19.590	17.162	20.978	22.753	
(n,2p)	6.052	8.470	10.711	8.907	13.500	17.111	
(n,d,n')	17.129	17.581	17.884	15.151	18.067	18.669	

Table 6(a)
Energy Levels for Hauser-Feshbach Calculations: ^{78}Kr

^{79}Kr		Residual Nucleus:					
		^{78}Kr		^{78}Br		^{75}Sc	
$\sigma_{n\gamma}$	I^π	$\sigma_{nn'}$	I^π	σ_{np}	I^π	σ_{na}	I^π
E (MeV)		E (MeV)		E (MeV)		E (MeV)	
0.000	$1/2^-$	0.000	0^+	0.000	1^+	0.000	$5/2^+$
0.300	$7/2^+$	0.455	2^+	0.032	2^-	0.110	$3/2^+$
0.147	$5/2^-$	1.119	4^+	0.180	4^+	0.285	$1/2^-$
0.183	$3/2^-$	1.978	6^-			0.420	$5/2^+$
0.291	$5/2^-$					0.610	$3/2^-$
0.384	$3/2^-$					0.750	$7/2^-$
0.402	$5/2^-$					0.860	$5/2^-$
0.450	$7/2^-$					0.903	$3/2^-$
0.534	$1/2^+$					1.030	$7/2^-$
0.660	$5/2^-$						
0.689	$5/2^+$						
0.695	$3/2^+$						
0.720	$7/2^-$						
0.810	$3/2^-$						
1.038	$7/2^-$						
1.912	$1/2^+$						
2.060	$3/2^+$						
2.768	$7/2^-$						

Table 6(b)
Energy Levels for Hauser-Feshbach Calculations: ^{80}Kr

^{81}Kr		Residual Nucleus:					
		^{80}Kr		^{80}Br		^{77}Sc	
$\sigma_{n\gamma}$	I^π	$\sigma_{nn'}$	I^π	σ_{np}	I^π	σ_{na}	I^π
E (MeV)		E (MeV)		E (MeV)		E (MeV)	
0.000	$7/2^+$	0.000	0^+	0.000	1^-	0.000	$1/2^-$
0.190	$1/2^-$	0.616	2^+	0.037	2^-	0.162	$7/2^+$
0.457	$3/2^-$	1.252	2^+	0.085	5^-	0.175	$9/2^+$
0.549	$1/2^+$	1.320	0^-	0.256	2^-	0.239	$3/2^-$
0.608	$5/2^-$	1.436	4^+	0.271	2^-	0.250	$5/2^-$
0.636	$7/2^-$	2.390	6^+	0.281	3^-	0.440	$5/2^-$
0.701	$3/2^+$	3.400	8^-	0.314	1^-	0.521	$3/2^+$
0.919	$3/2^-$			0.366	1^-	0.680	$5/2^-$
1.025	$3/2^+$			0.381	3^+	0.818	$1/2^+$
1.108	$1/2^+$			0.468	1^-	0.912	$3/2^+$
1.280	$3/2^+$			0.684	2^+	0.956	$1/2^-$
1.677	$5/2^+$			0.722	1^+	1.006	$3/2^+$
1.803	$3/2^-$			0.760	1^-	1.126	$1/2^-$
				0.835	1^+	1.412	$1/2^-$
				1.139	1^-	1.623	$1/2^-$
				1.200	2^-	1.819	$1/2^-$
				1.410	3^-	2.393	$3/2^-$
				1.700	2^-		
				1.880	2^-		

Table 6(c)
Energy Levels for Hauser-Feshbach Calculations: ^{82}Kr

^{83}Kr			Residual Nucleus: ^{82}Br				^{79}Sc				
$\sigma_{n\gamma}$	E (MeV)	I^π	$\sigma_{nn'}$	E (MeV)	I^π	σ_{np}	E (MeV)	I^π	σ_{nd}	E (MeV)	I^π
0.000	9/2 ⁺		0.000	0 ⁺		0.000	5 ⁻		0.000	7/2 ⁺	
0.009	7/2 ⁺		0.777	2 ⁺		0.046	2 ⁻		0.096	1/2 ⁻	
0.042	1/2 ⁻		1.475	2 ⁺		0.078	1 ⁺		0.130	9/2 ⁺	
0.562	5/2 ⁻		1.820	4 ⁺					0.365	5/2 ⁻	
0.571	3/2 ⁻		2.094	3 ⁺					0.526	1/2 ⁻	
0.690	3/2 ⁺		2.172	0 ⁺					0.620	3/2 ⁺	
0.798	7/2 ⁻		2.427	3 ⁺					0.720	3/2 ⁻	
			2.648	4 ⁻					0.974	1/2 ⁻	
			2.828	5 ⁻					1.160	1/2 ⁺	
			2.920	6 ⁺					1.490	1/2 ⁺	
									1.670	3/2 ⁺	
									2.040	1/2 ⁻	
									2.280	3/2 ⁻	
									2.590	3/2 ⁺	
									2.960	1/2 ⁺	
									3.280	1/2 ⁺	
									3.440	3/2 ⁺	

Table 6(d)
Energy Levels for Hauser-Feshbach Calculations: ^{83}Kr

^{84}Kr			Residual Nucleus: ^{83}Br				^{80}Sc				
$\sigma_{n\gamma}$	E (MeV)	I^π	$\sigma_{nn'}$	E (MeV)	I^π	σ_{np}	E (MeV)	I^π	σ_{nd}	E (MeV)	I^π
0.000	0 ⁺		0.000	9/2 ⁺		0.000	3/2 ⁻		0.000	0 ⁺	
0.882	2 ⁺		0.009	7/2 ⁺		0.357	5/2 ⁻		0.686	2 ⁺	
1.834	0 ⁺		0.042	1/2 ⁻		0.988	1/2 ⁻		1.449	2 ⁺	
1.900	2 ⁺		0.562	5/2 ⁻		1.030	3/2 ⁻		1.479	0 ⁺	
2.086	4 ⁺		0.571	3/2 ⁻		1.700	1/2 ⁻		1.960	2 ⁺	
2.337	4 ⁺		0.690	5/2 ⁻		2.050	3/2 ⁻		2.310	2 ⁺	
2.705	3 ⁻		0.798	7/2 ⁻		2.450	7/2 ⁺		2.514	2 ⁺	
2.775	2 ⁺					2.646	7/2 ⁺		2.814	2 ⁺	
3.048	4 ⁺					2.738	1/2 ⁺		3.126	2 ⁺	
3.225	1 ⁻					2.946	7/2 ⁻		3.248	2 ⁺	
3.477	1 ⁻					3.09	1/2 ⁻		3.350	1 ⁺	
3.570	3 ⁻								3.390	2 ⁺	
3.650	5 ⁻								4.063	0 ⁺	
3.721	3 ⁻										

*Reference 24.

Table 6(e)
Energy Levels for Hauser-Feshbach Calculations: ^{84}Kr

^{85}Kr		Residual Nucleus:				^{81}Sc	
E (MeV)	$\sigma_{n\gamma}^*$	^{84}Kr		^{84}Br		^{81}Sc	
	I^π	E (MeV)	I^π	E (MeV)	I^π	E (MeV)	I^π
0.000	$9/2^+$	0.000	0^-	0.000	2^-	0.000	$1/2^-$
0.305	$1/2^-$	0.822	2^+	0.408	1^-	0.103	$7/2^+$
1.050	$3/2^-$	1.834	0^+	0.557	6^-	0.294	$9/2^-$
1.230	$5/2^-$	1.900	2^+	0.873	2^-	0.468	$1/2^-$
1.767	$3/2^+$	2.086	4^+	0.979	3^-	0.625	$5/2^+$
2.108	$1/2^-$	2.337	4^+	1.196	4^-	1.053	$3/2^+$
2.166	$1/2^+$	2.705	3^-			1.232	$1/2^+$
2.237	$7/2^+$	2.775	2^+			1.303	$3/2^-$
2.418	$5/2^-$	3.048	4^-			1.406	$1/2^+$
3.380	$7/2^-$	3.225	1^-			1.725	$3/2^+$
		3.477	1^-			1.828	$5/2^+$
		3.570	3^-			2.174	$3/2^+$
		3.650	5^-			2.550	$5/2^+$
		3.721	3^-			2.680	$1/2^+$
						3.070	$3/2^+$
						3.310	$5/2^+$
						3.490	$3/2^+$
						3.570	$1/2^+$
						3.670	$3/2^+$
						3.720	$5/2^+$

*Reference 23.

Table 6(f)
Energy Levels for Hauser-Feshbach Calculations: ^{86}Kr

^{87}Kr		Residual Nucleus:				^{83}Sc	
E (MeV)	$\sigma_{n\gamma}^*$	^{86}Kr		^{86}Br		^{83}Sc	
	I^π	E (MeV)	I^π	E (MeV)	I^π	E (MeV)	I^π
0.000	$5/2^+$	0.000	0^+	0.000	2^-	0.000	$9/2^+$
0.529	$1/2^+$	1.563	2^+	0.196	1^-	0.220	$1/2^-$
1.468	$3/2^+$	2.248	4^+	0.268	4^-	1.050	$3/2^-$
1.873	$5/2^+$	2.355	2^+	0.390	2^-	1.230	$5/2^-$
1.996	$3/2^+$	2.733	0^+	0.862	1^-	1.767	$3/2^-$
2.080	$5/2^+$	3.109	3^-	1.210	1^+	2.108	$1/2^+$
2.112	$3/2^+$	3.542	0^+	2.232	1^+	2.166	$1/2^+$
2.250	$9/2^-$	3.832	0^+	2.392	1^+	2.237	$7/2^-$
2.277	$1/2^+$	3.959	4^+	2.772	1^-	2.418	$5/2^-$
2.515	$7/2^+$	4.111	2^+			3.380	$7/2^-$
2.775	$3/2^+$	4.194	2^-				
2.825	$3/2^+$	4.298	3^+				
3.015	$5/2^+$	4.668	4^+				
3.223	$3/2^+$	4.826	2^+				
3.237	$5/2^+$	4.948	2^-				

*References 23 and 25.

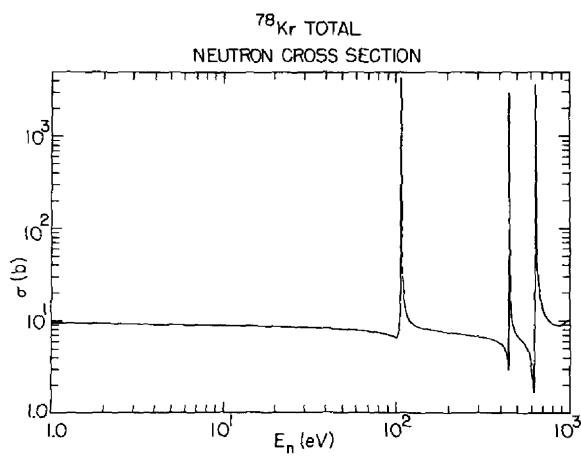


Figure 1.

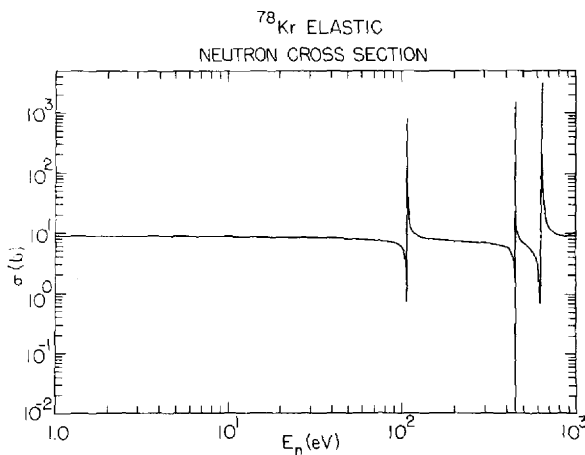


Figure 2.

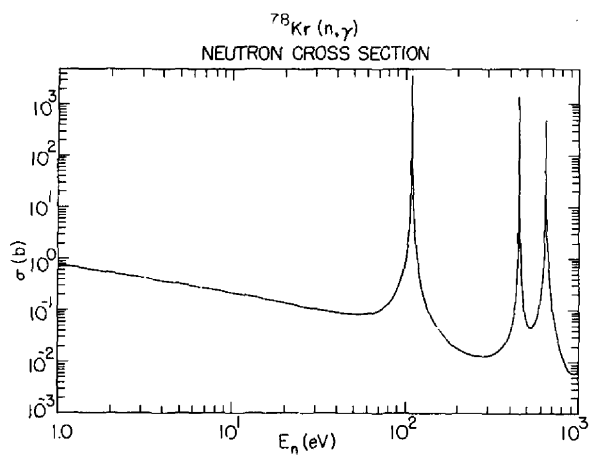


Figure 3.

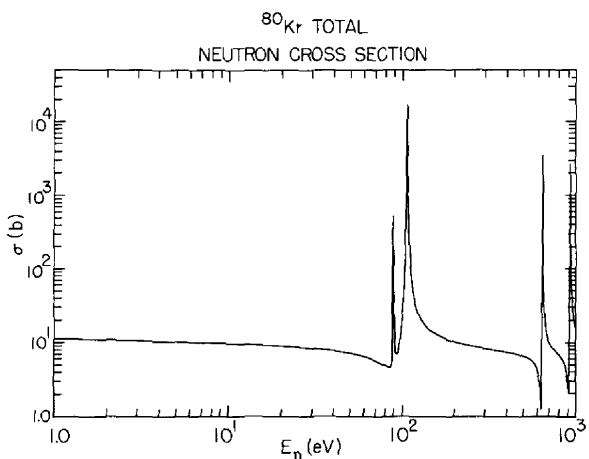


Figure 4.

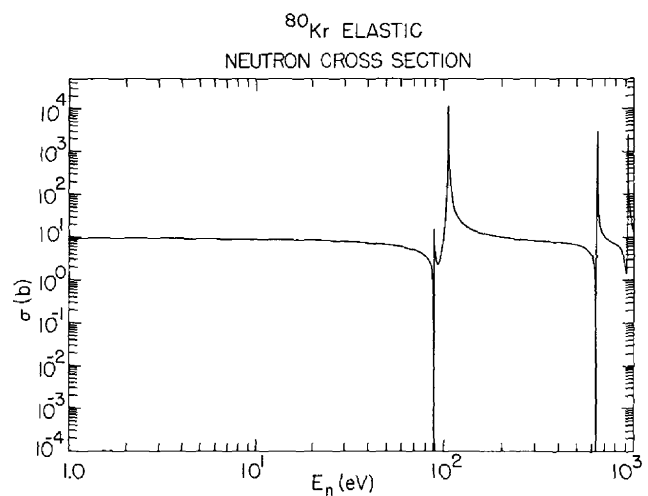


Figure 5.

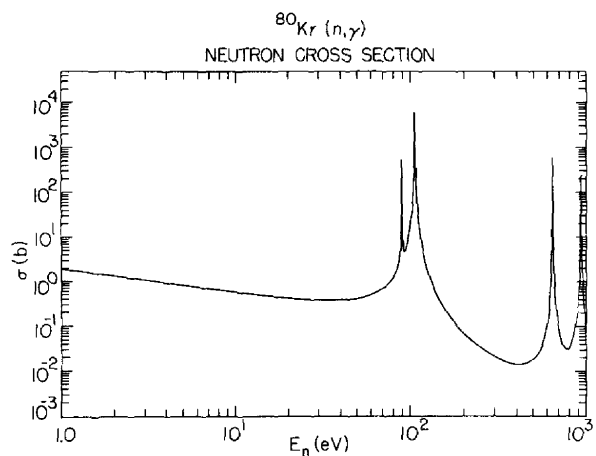


Figure 6.

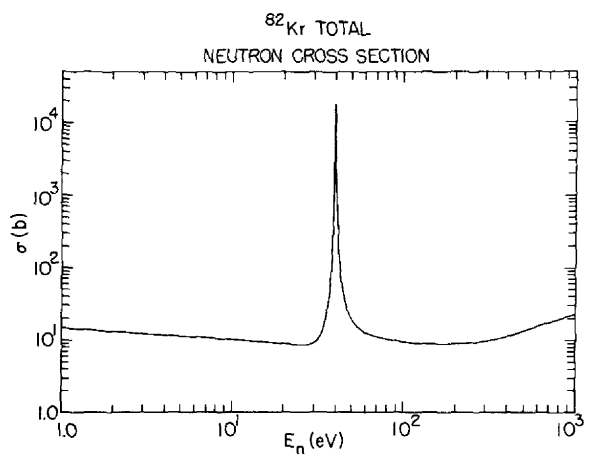


Figure 7.

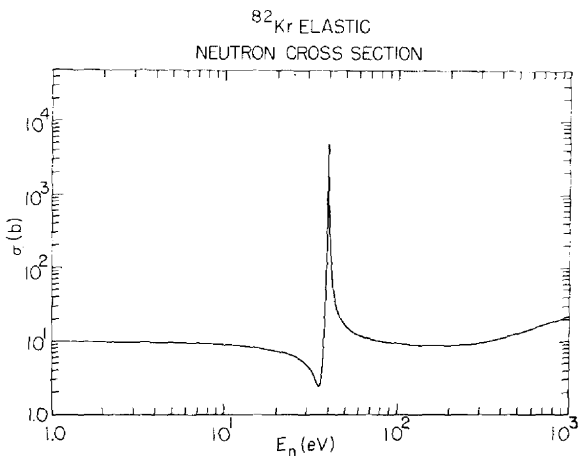


Figure 8.

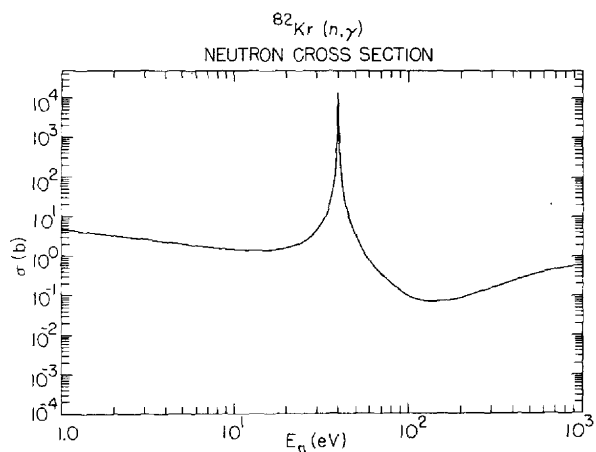


Figure 9.

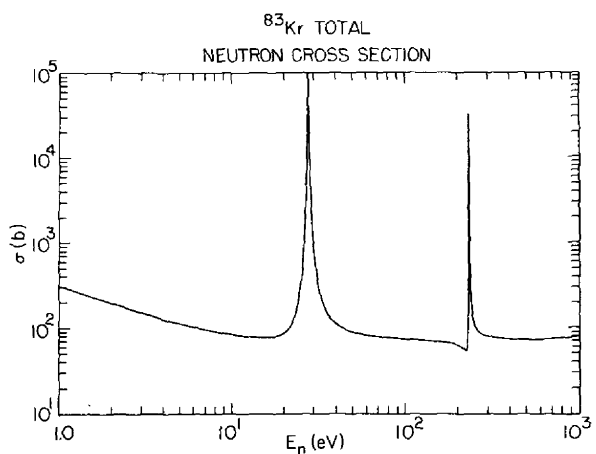


Figure 10.

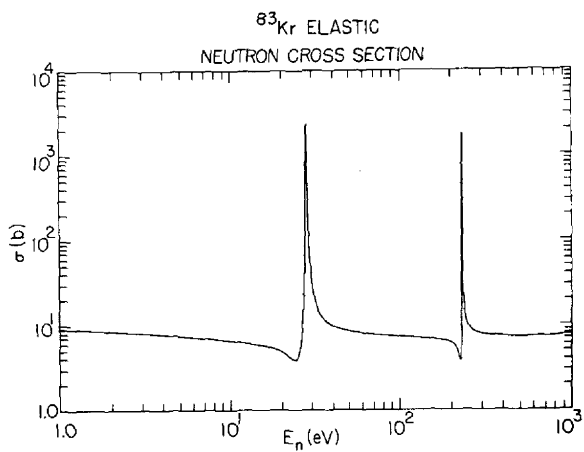


Figure 11.

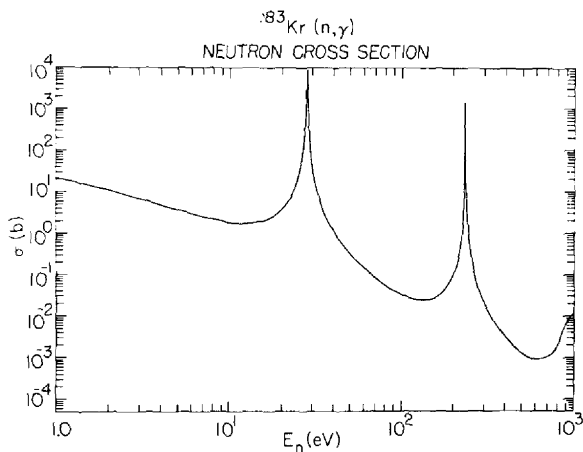


Figure 12.

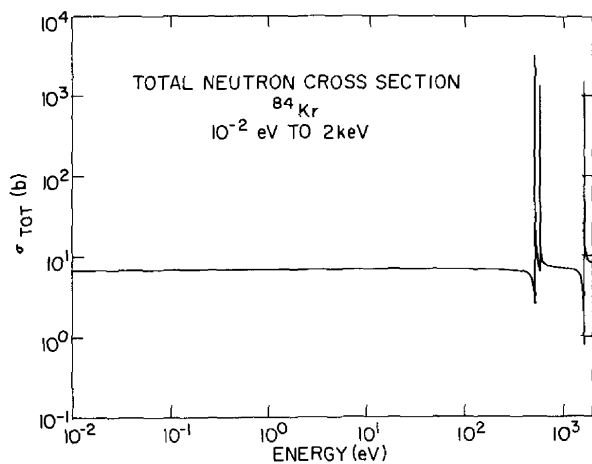


Figure 13.

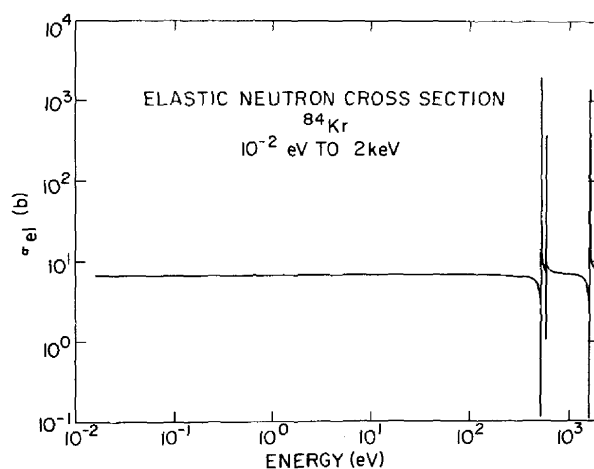


Figure 14.

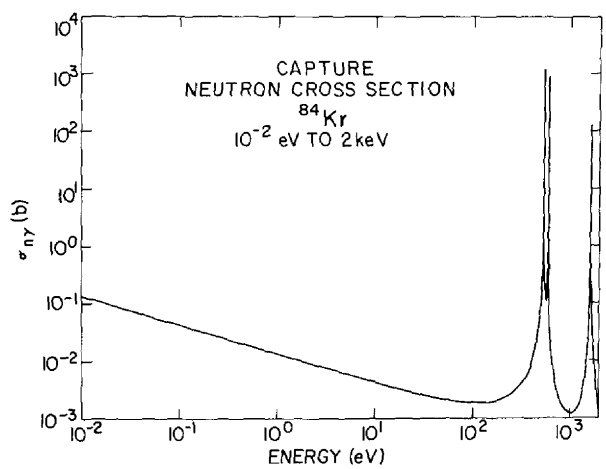


Figure 15.

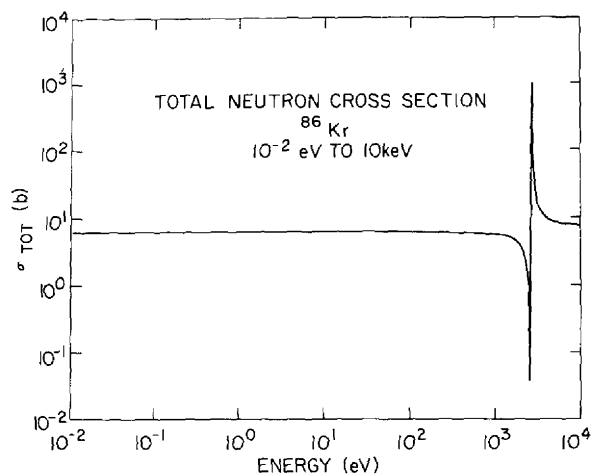


Figure 16.

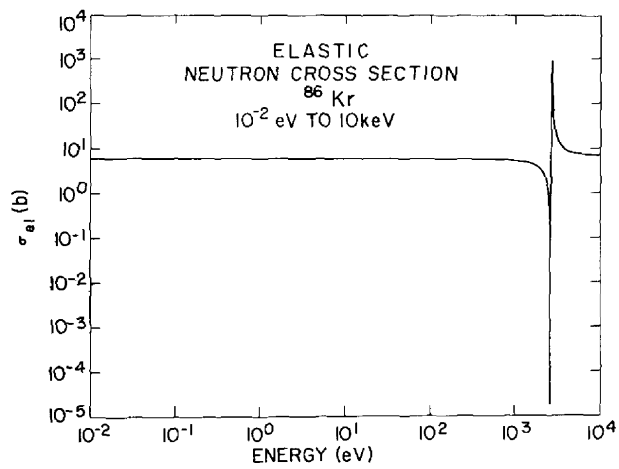


Figure 17.

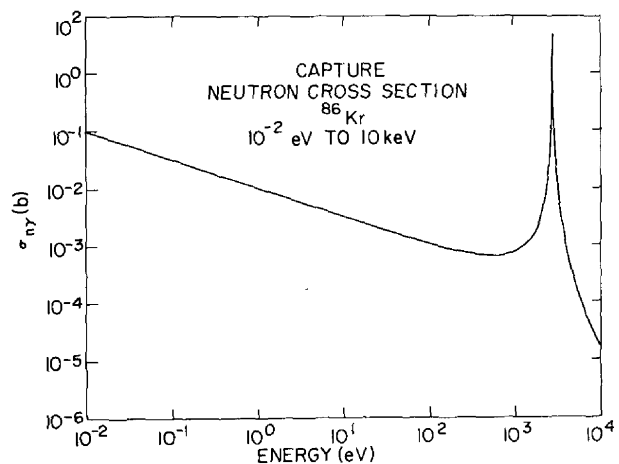


Figure 18.

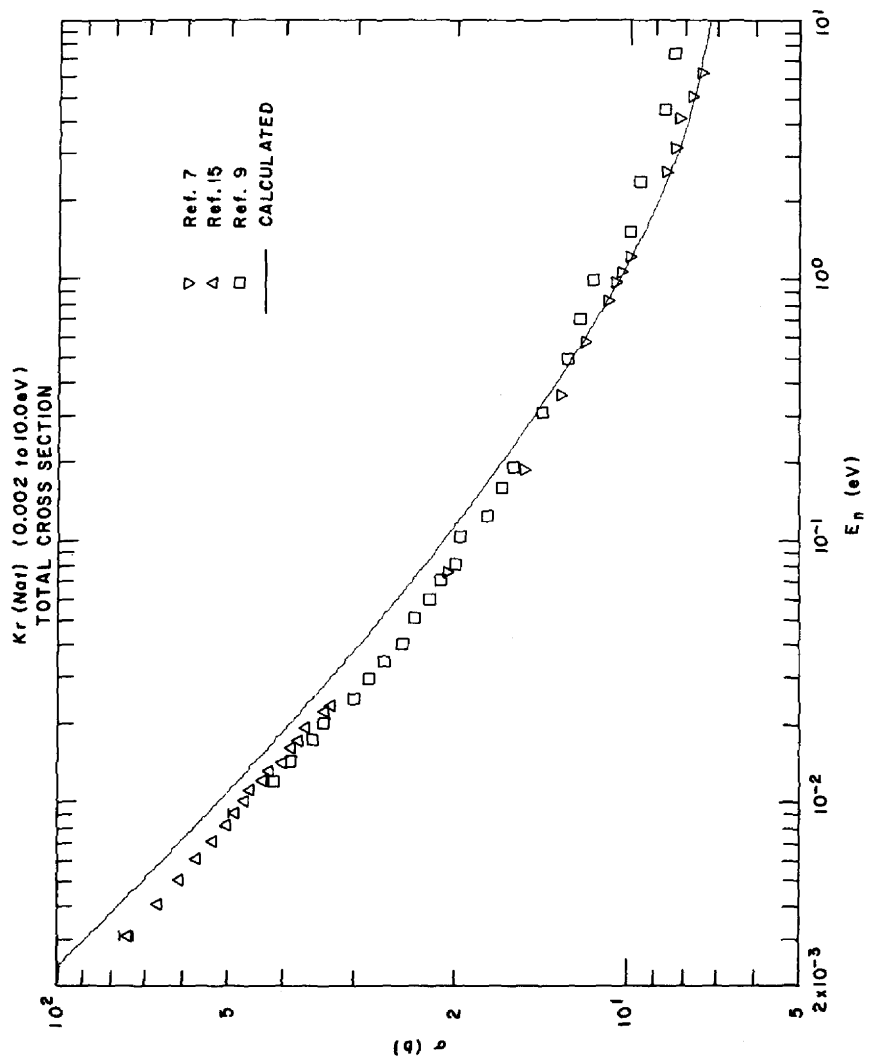


Figure 19.

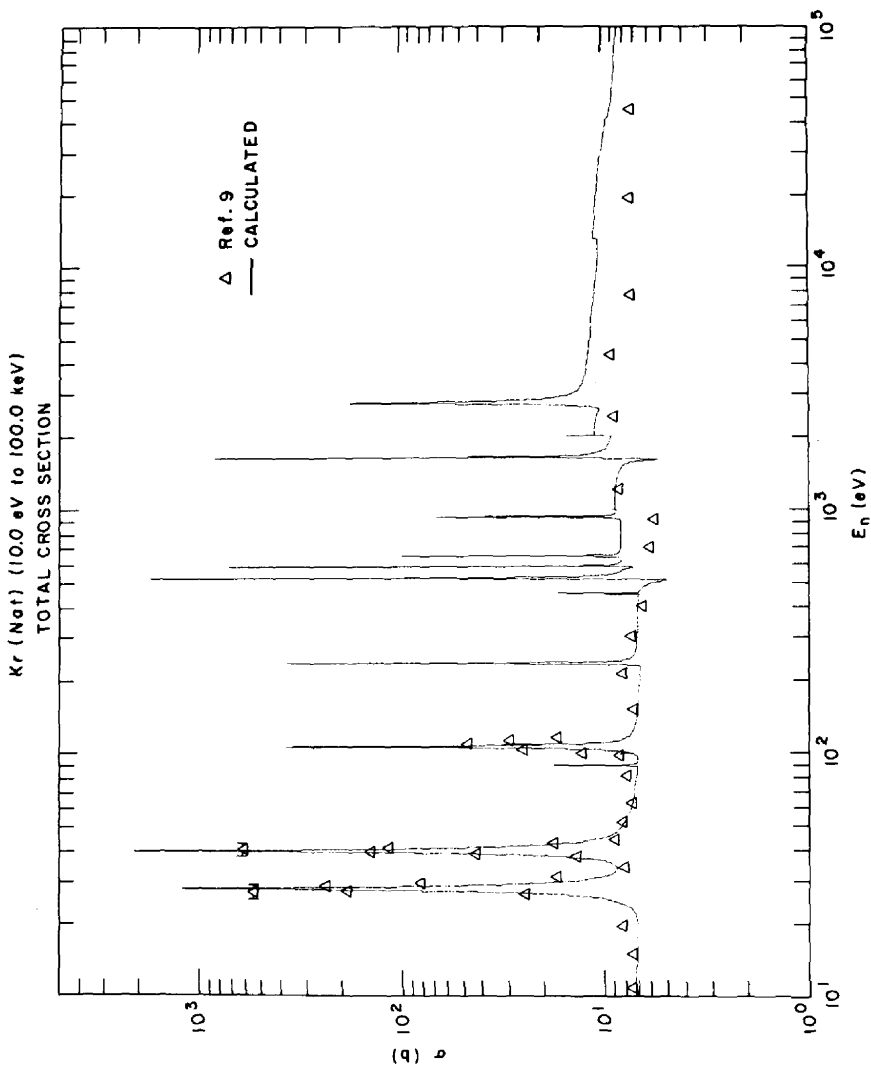


Figure 20.

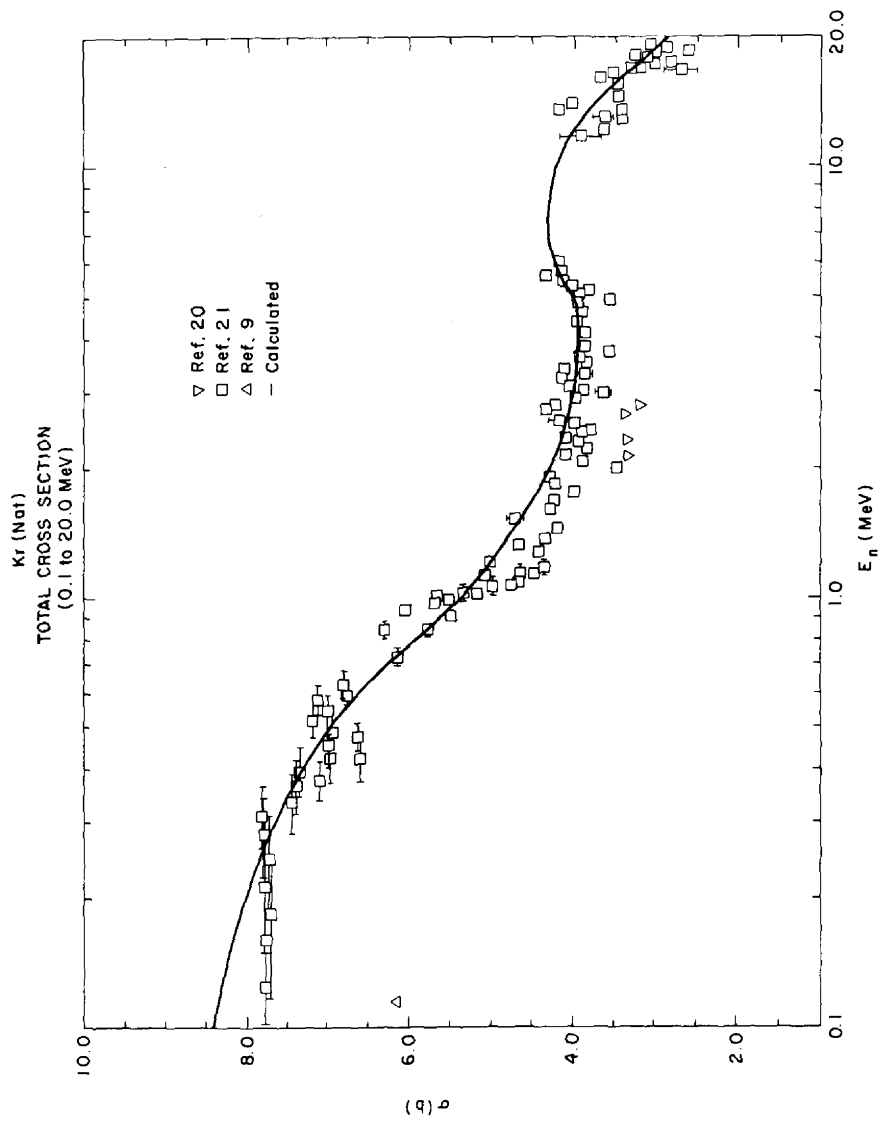


Figure 21.

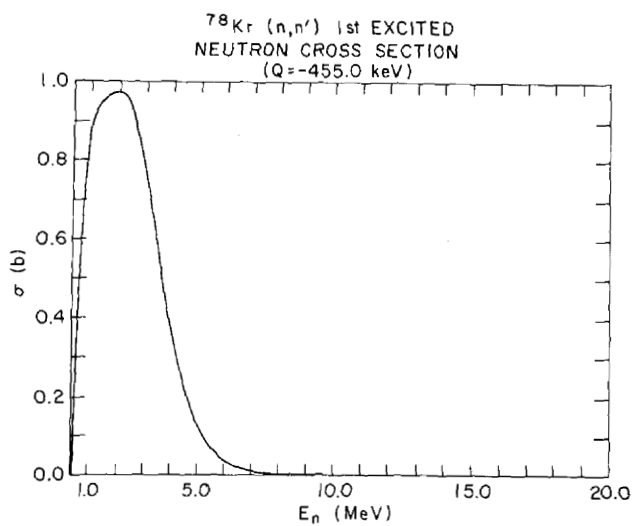


Figure 22.

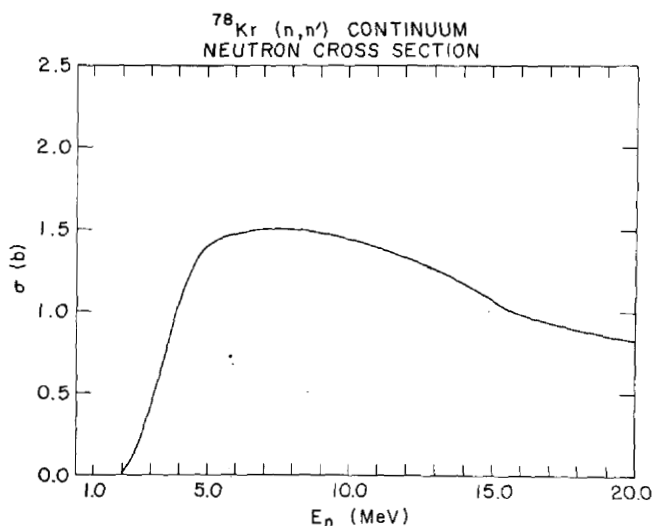


Figure 23.

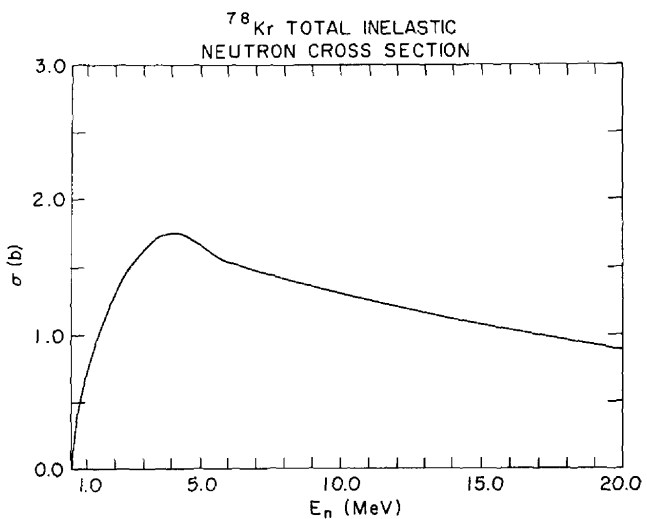


Figure 24.

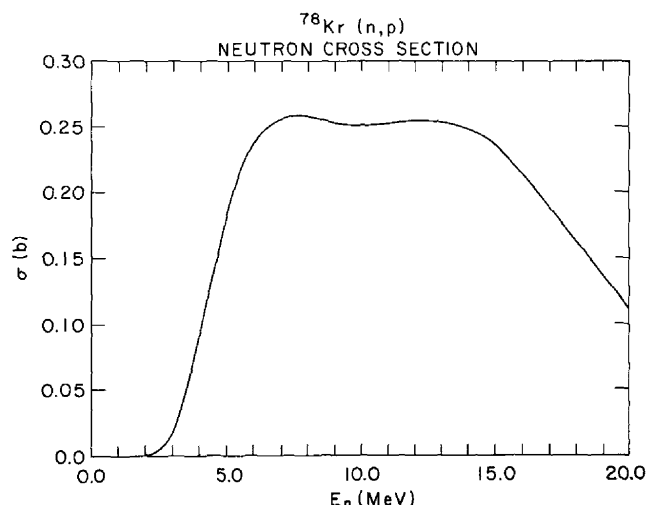


Figure 25.

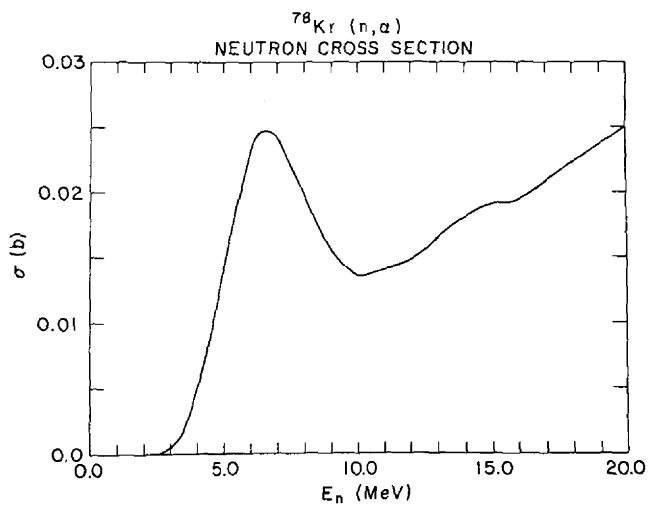


Figure 26.

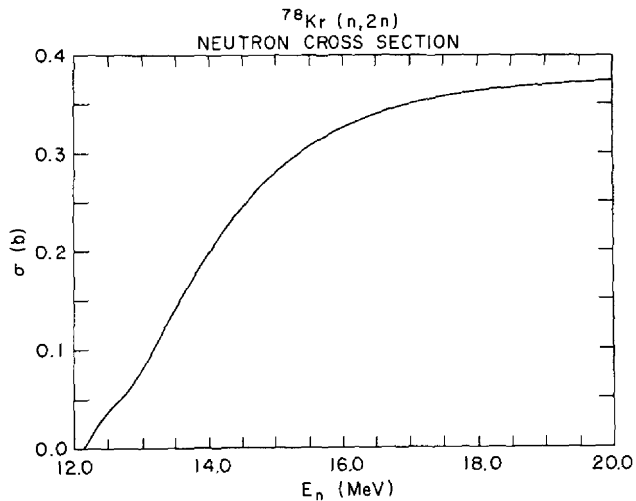


Figure 27.

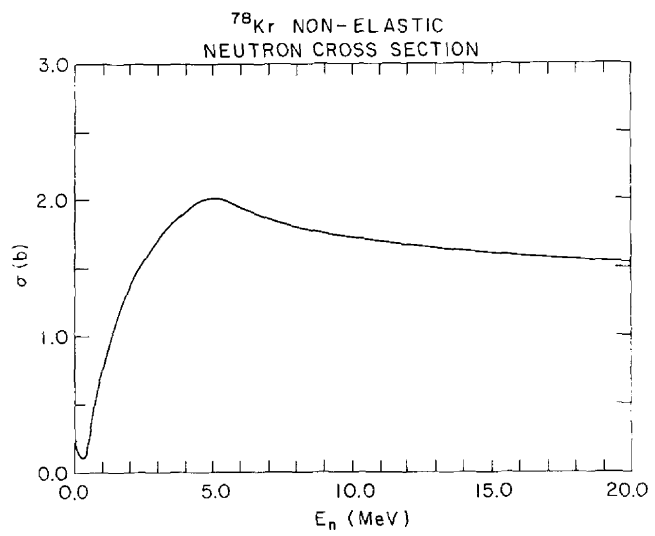


Figure 28.

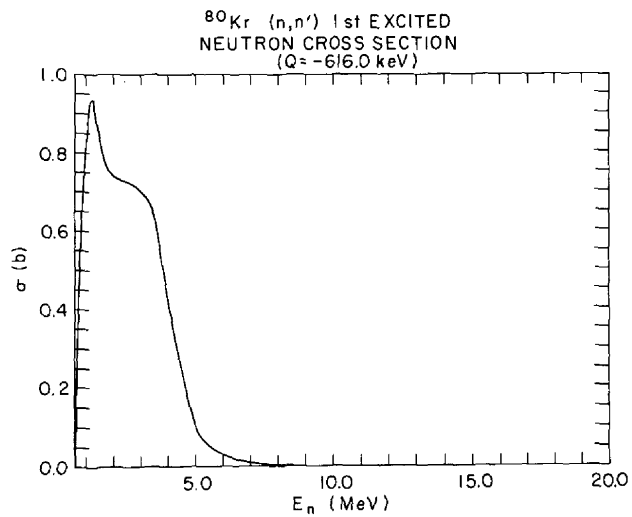


Figure 29.

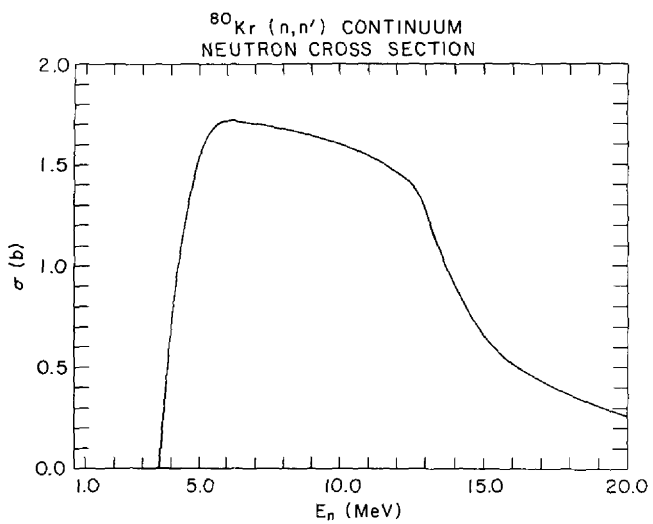


Figure 30.

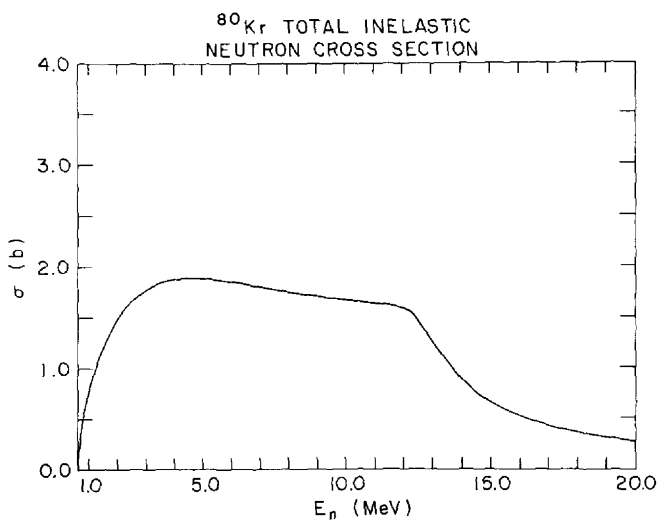


Figure 31.

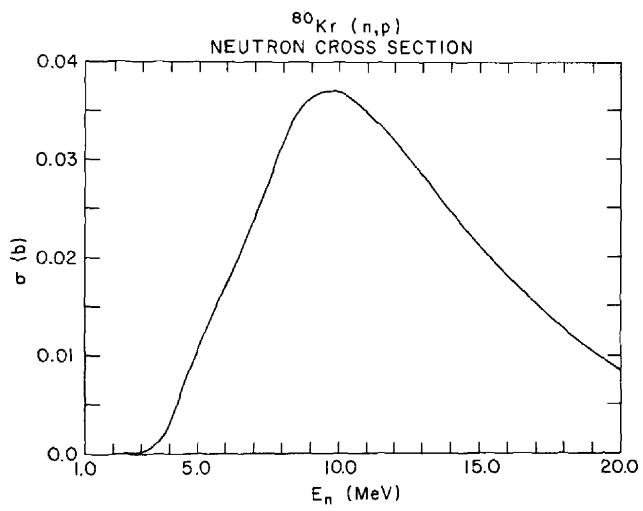


Figure 32.

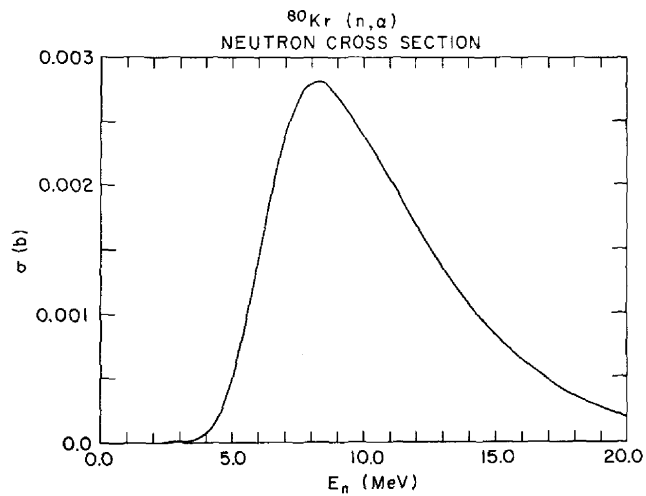


Figure 33.

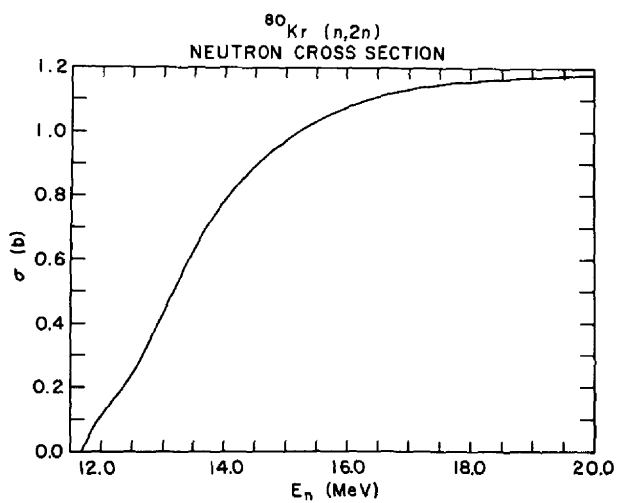


Figure 34.

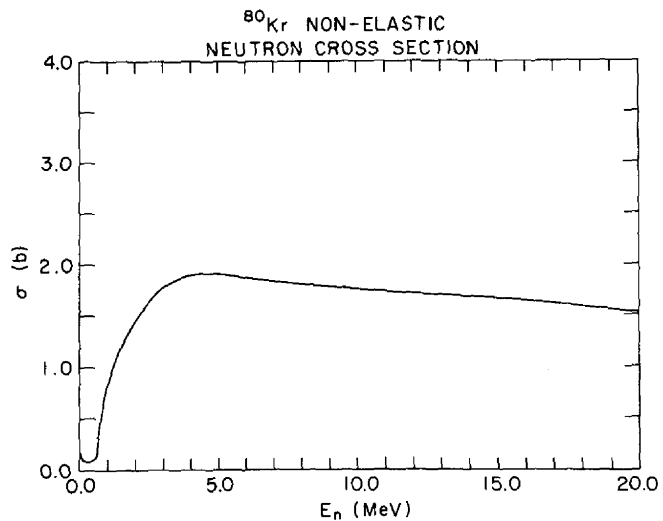


Figure 35.

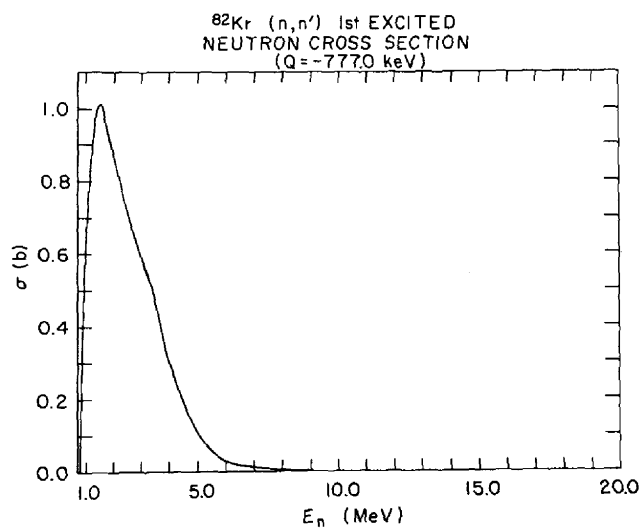


Figure 36.

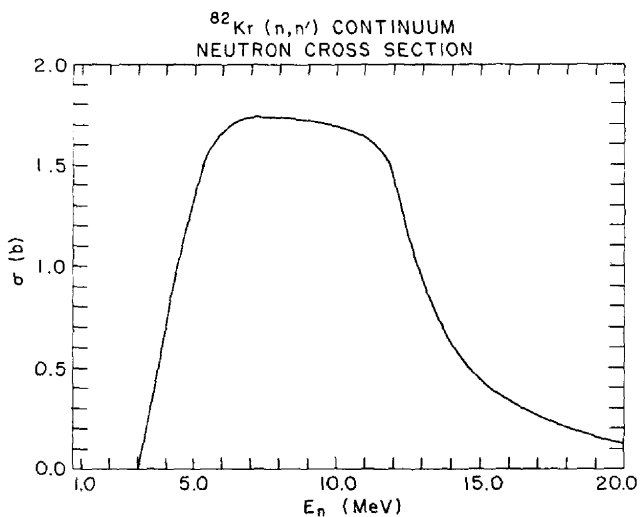


Figure 37.

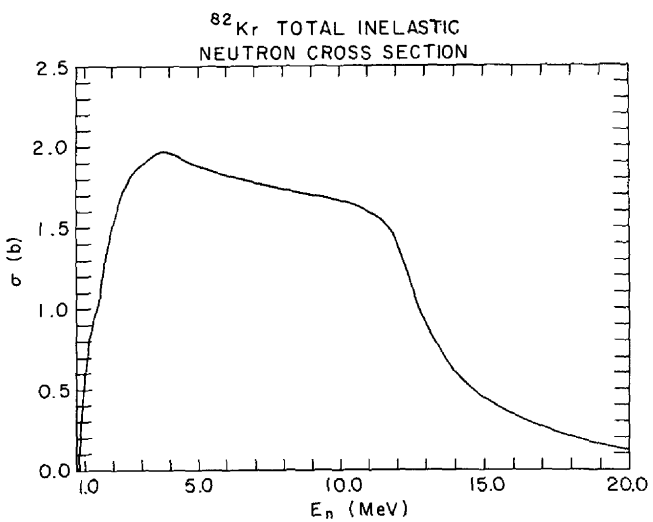


Figure 38.

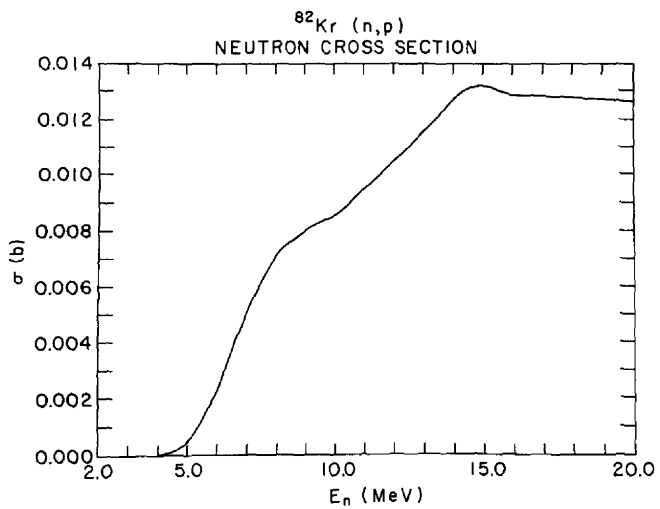


Figure 39.

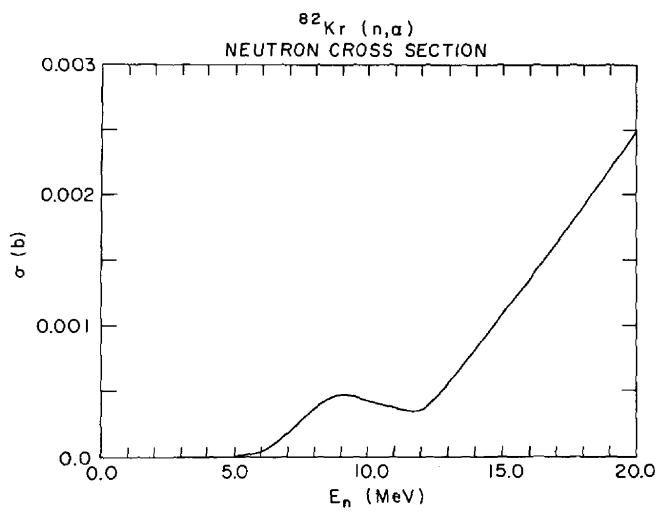


Figure 40.

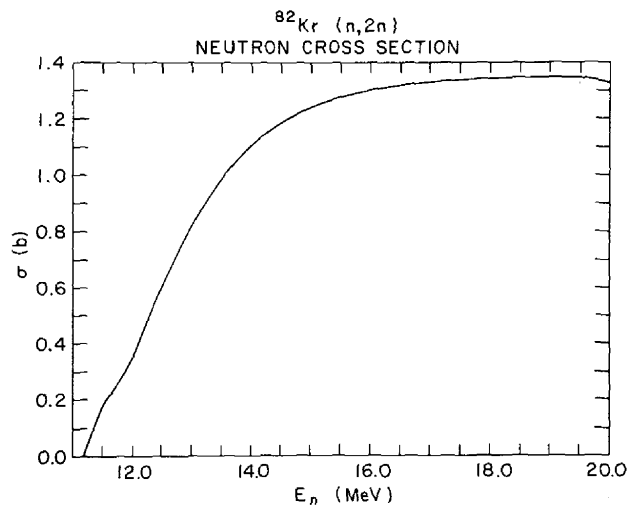


Figure 41.

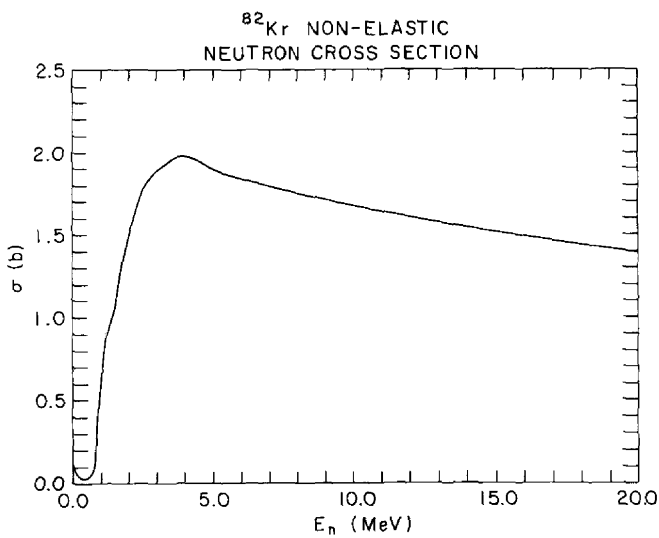


Figure 42.

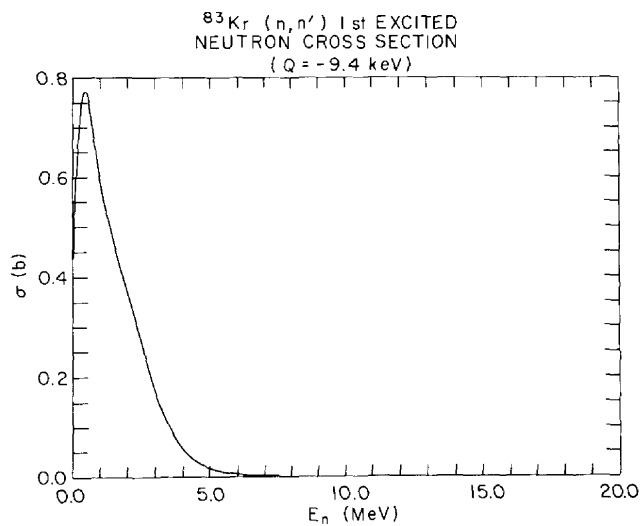


Figure 43.

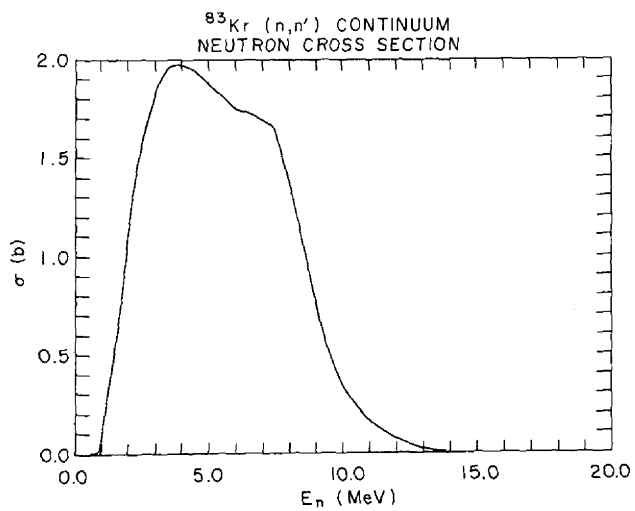


Figure 44.

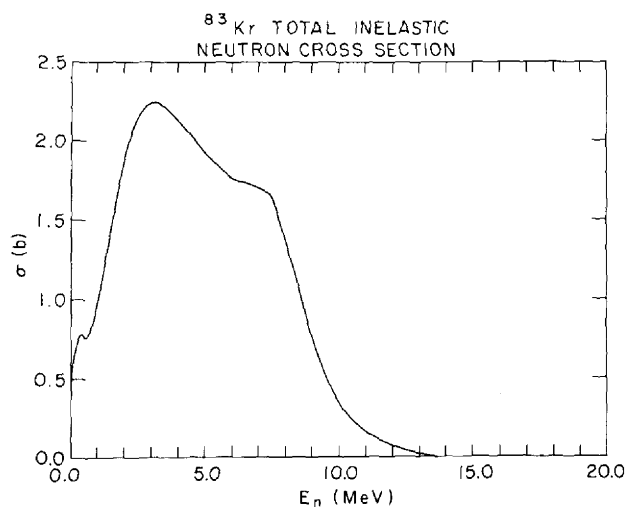


Figure 45.

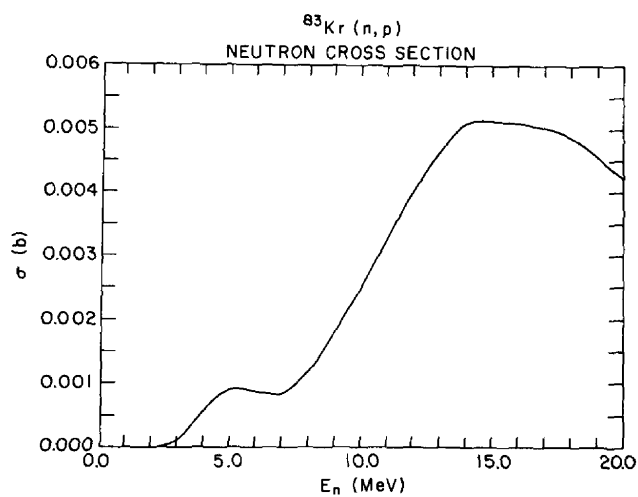


Figure 46.

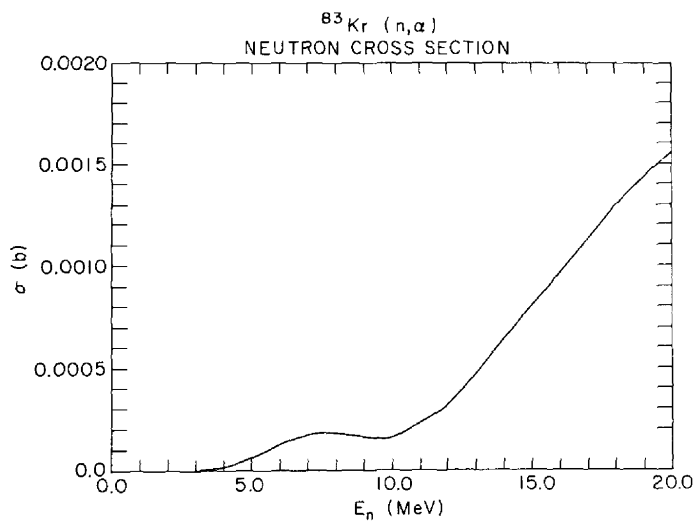


Figure 47.

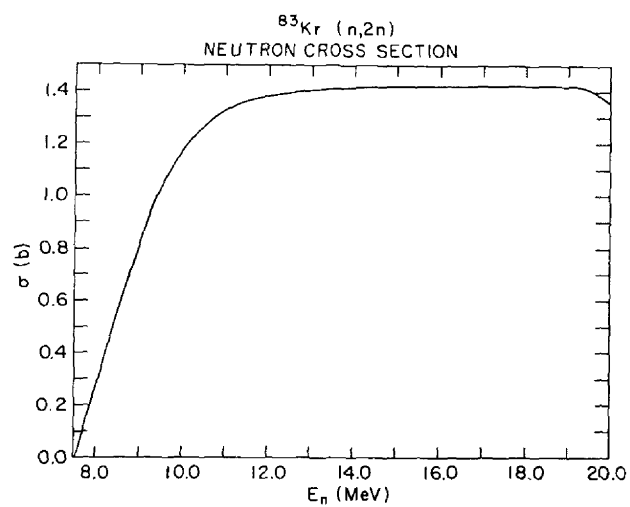


Figure 48.

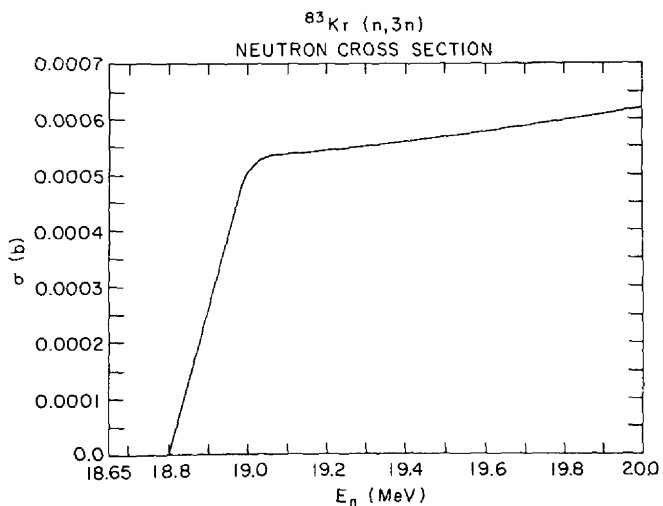


Figure 49.

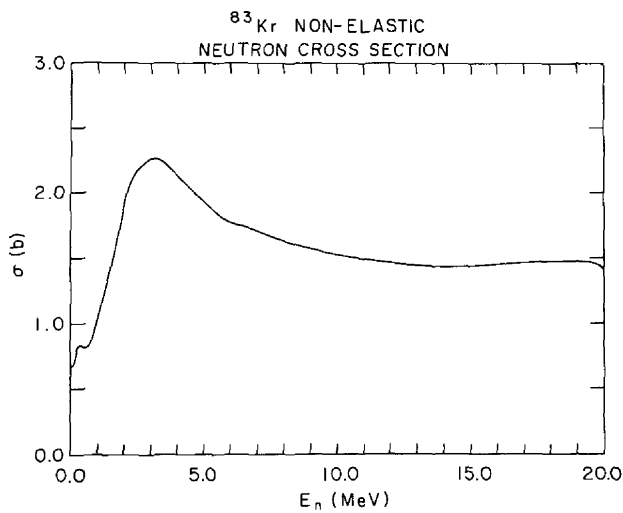


Figure 50.

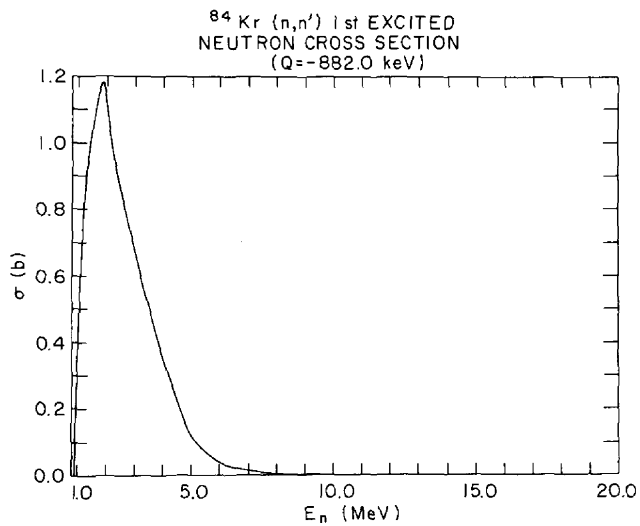


Figure 51.

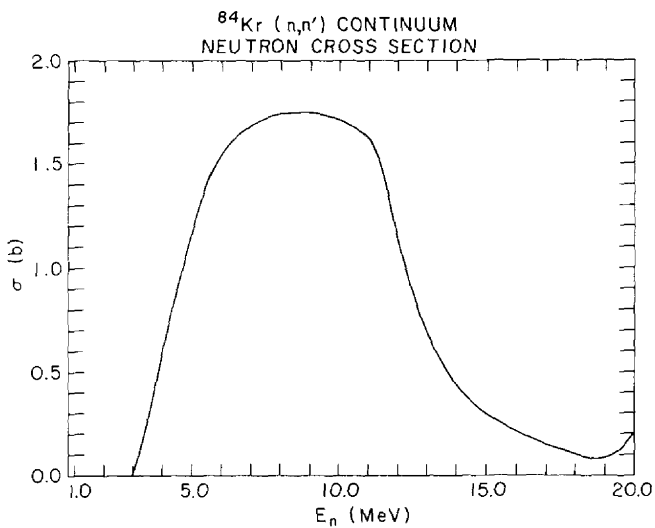


Figure 52.

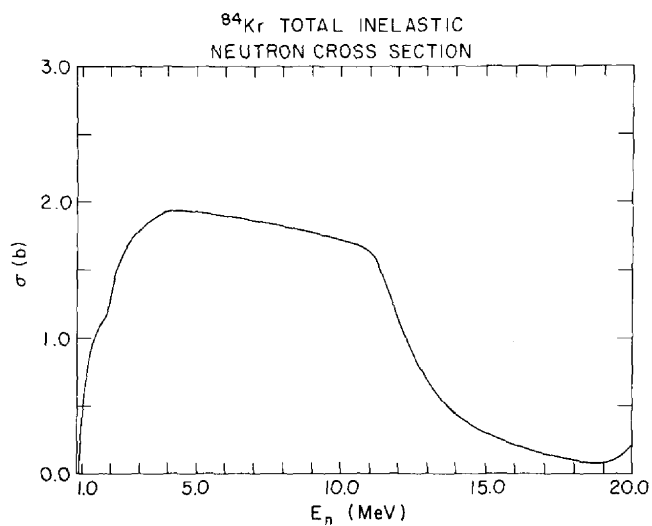


Figure 53.

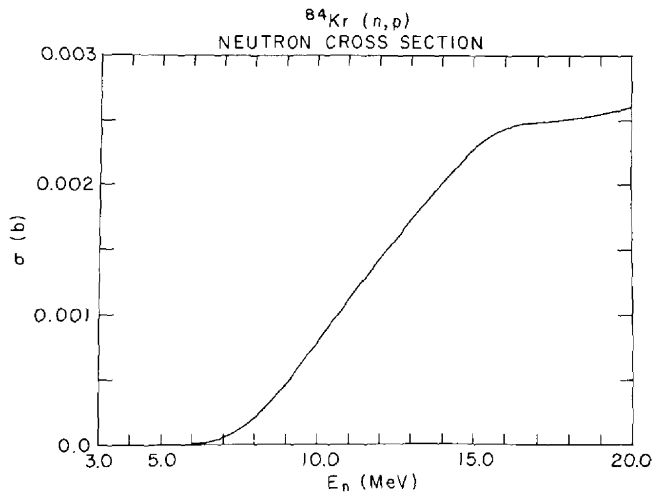


Figure 54.

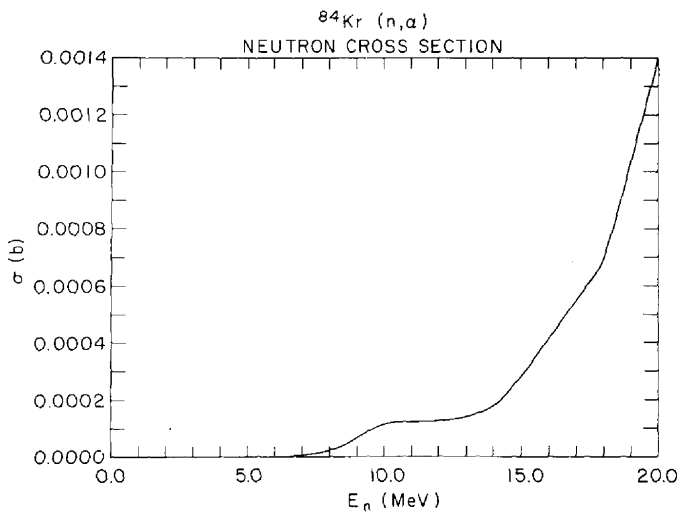


Figure 55.

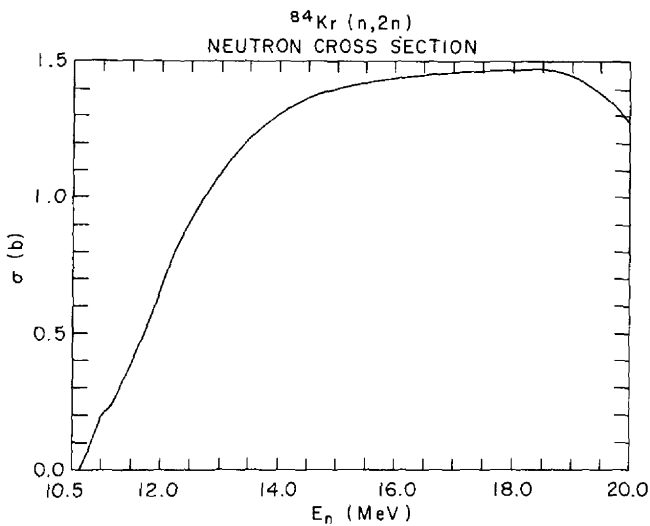


Figure 56.

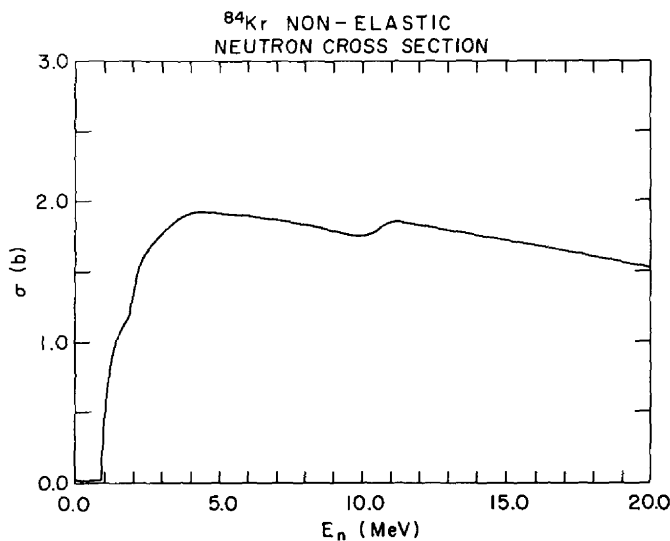


Figure 57.

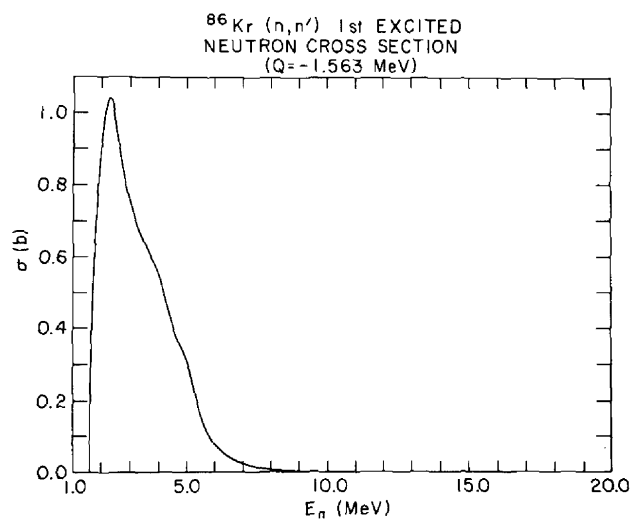


Figure 58.

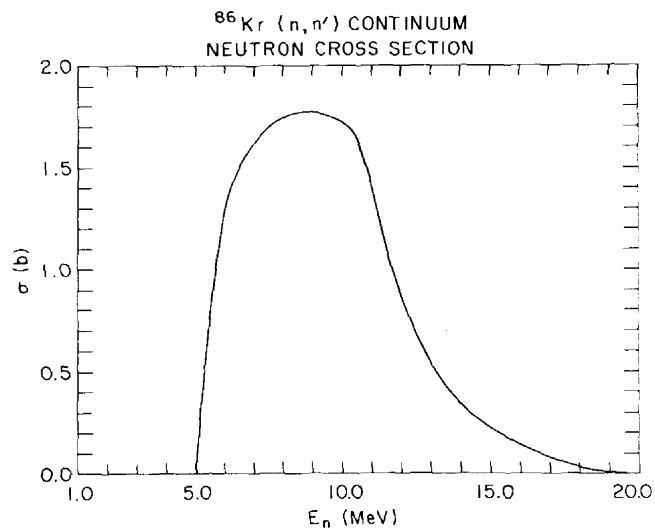


Figure 59.

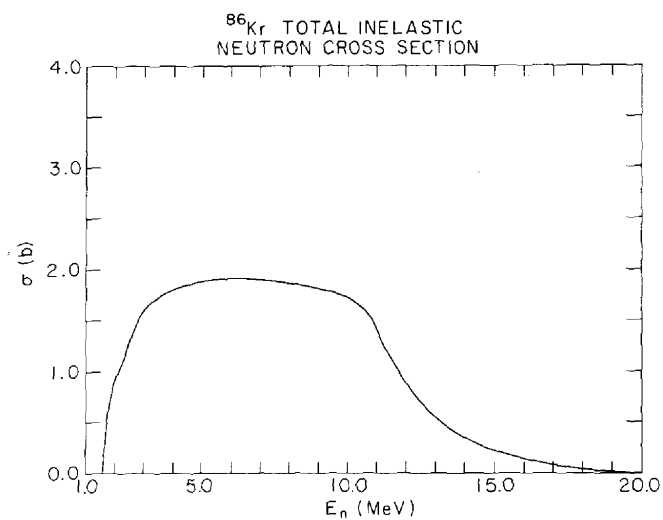


Figure 60.

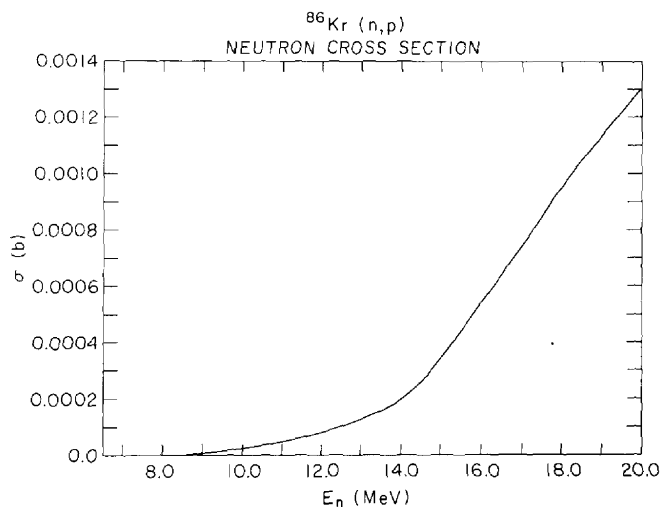


Figure 61.

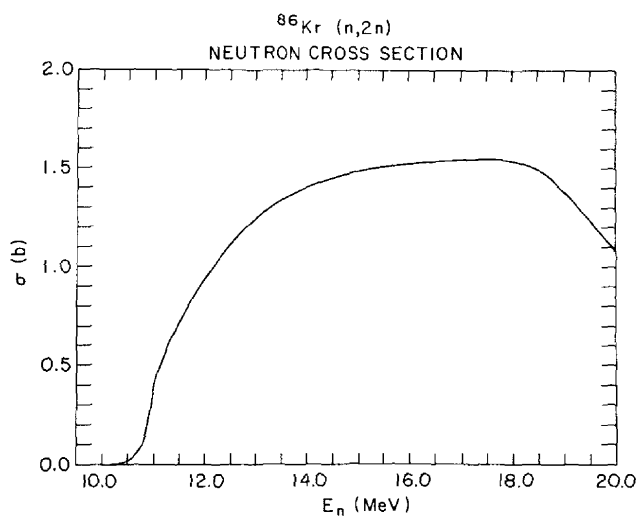


Figure 62.

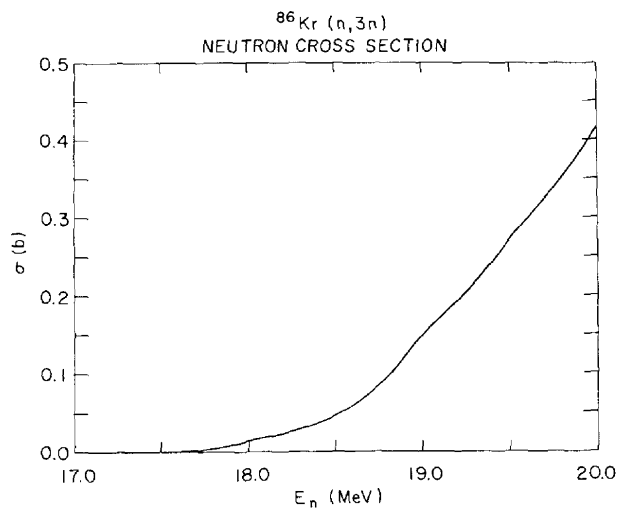


Figure 63.

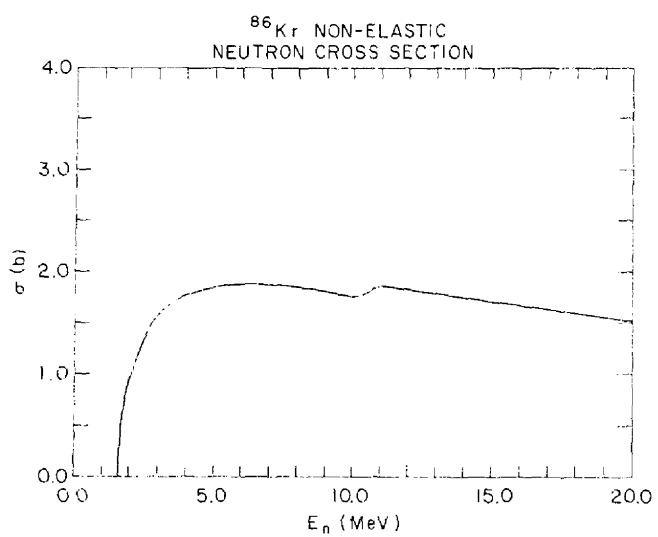


Figure 64.

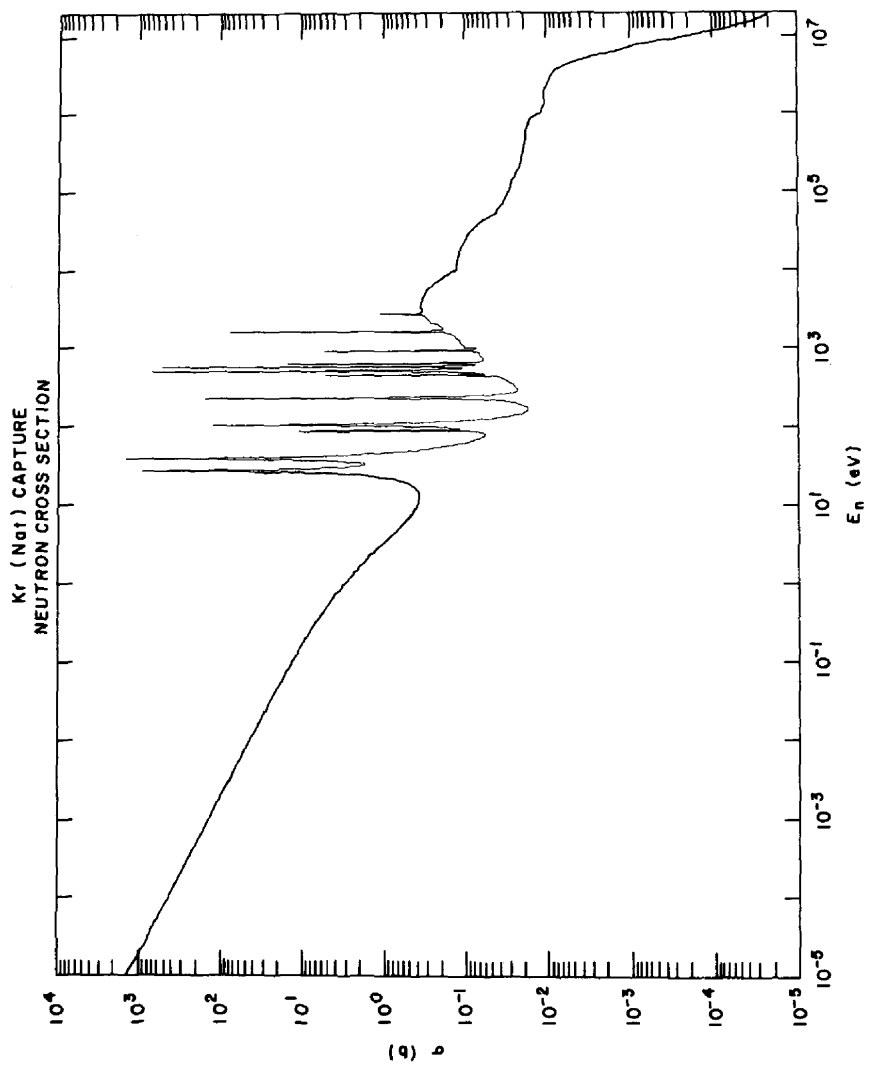


Figure 65.

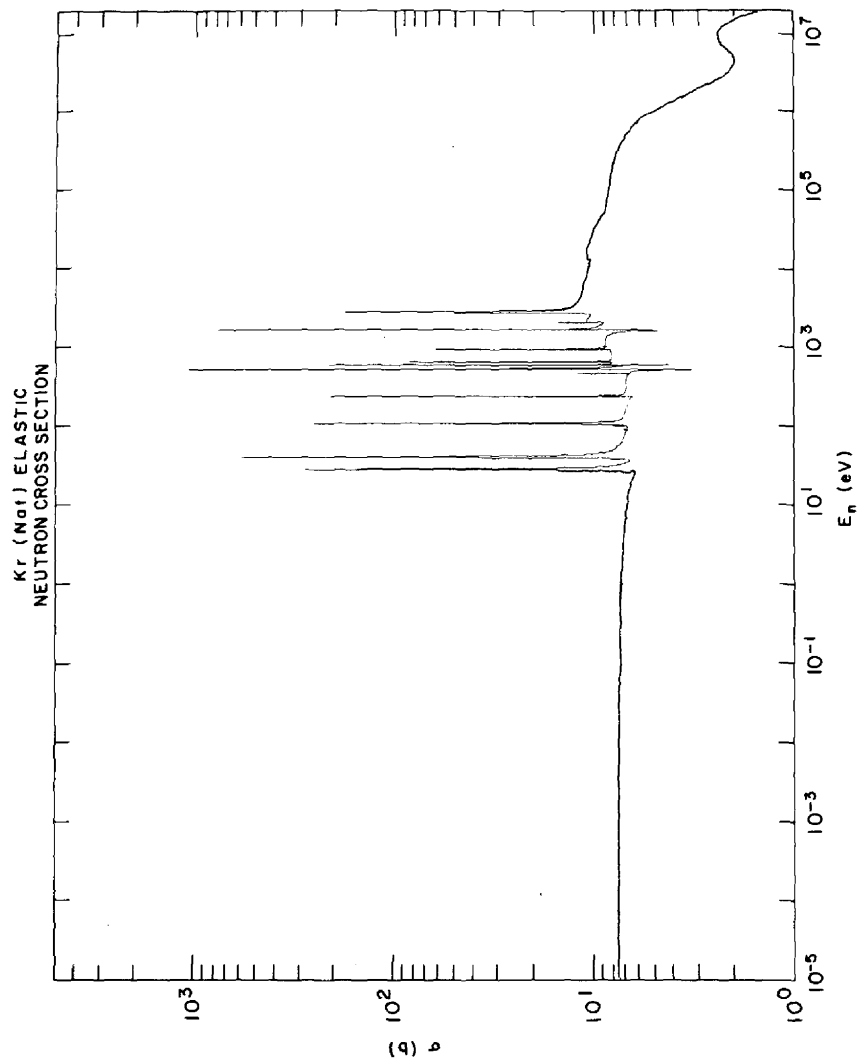


Figure 66.

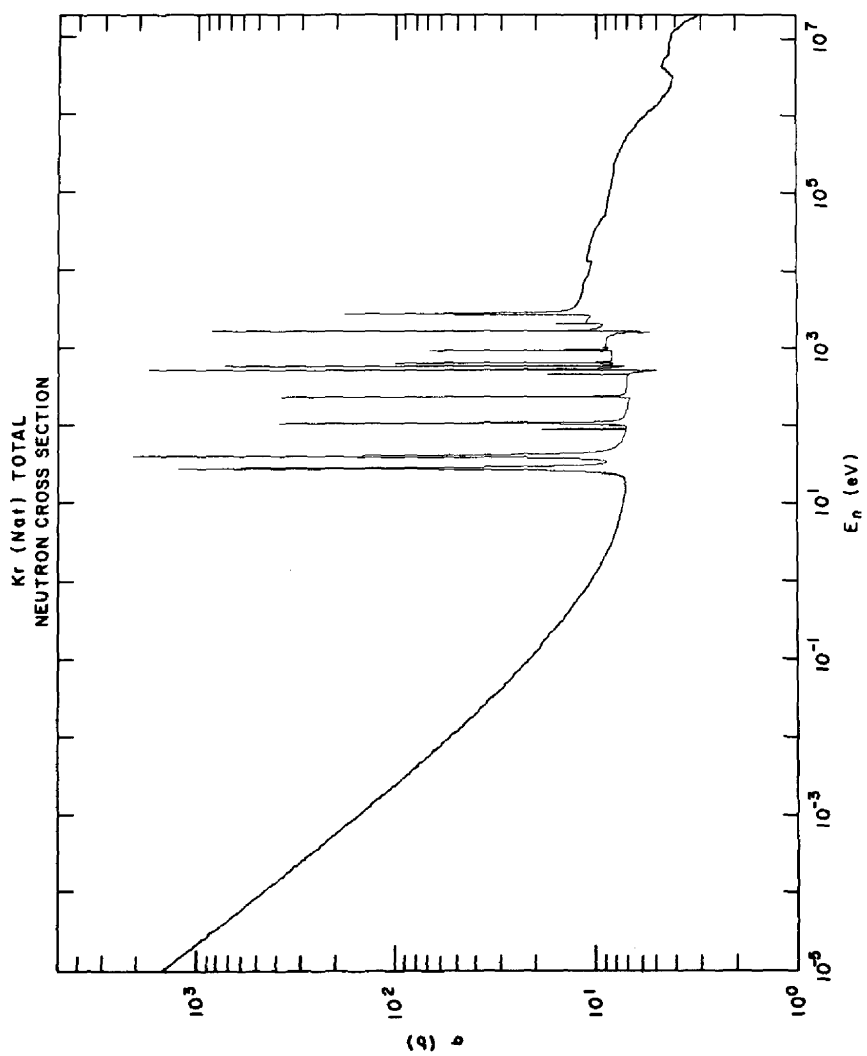


Figure 67.

